Jukka Koivunen

Characterisation of MIMO Propagation Channel in Multi-link Scenarios

Thesis submitted in partial fulfillment for the degree of Master of Science in Espoo _____,_____

Supervisor	Professor	Pertti Vainikainen
Instructor	M.Sc	Veli-Matti Kolmonen

Abstract

Helsinki University of Technology — Abstract of the Master's Thesis

Author:	Jukka Koivunen		
Name of the Thesis:	Characterisation of MIMO Propagation Channel in Multi-link Scenarios		
Date:	December 10, 2007	Number of Pages:	67
Department:	Department of Electrical and Communications Engineering		
Professorship:	S-26 Radio Engineering		
Supervisor:	Professor Pertti Vainikainen		
Instructor:	M.Sc. Veli-Matti Kolmonen		

In this master's thesis a measurement system for dynamic wideband double directional multi-link MIMO propagation measurements at 5.3 GHz was developed. The system is able to measure two 32x32 MIMO channels simultaneously with maximum doppler frequency of 11.73 Hz. Two measurement campaigns using this system were conducted, and measurement data from the campaigns were analyzed to verify the correct operation of the system.

The literal part of the work begun with a literature review on existing MIMO channel models and MIMO channel sounding measurements. In this survey it was seen that no dynamic MIMO multi-link measurements have been performed previously. Also the basics of the MIMO systems and MIMO propagation channel measurement technigues were studied.

The possible configurations for measuring the multi-link MIMO channel were considered and a system based on two existing channel sounding equipment was presented. The interoperability of the sounders was made possible with some system modifications done to the TKK sounder.

Finally it was shown that the measurement system is able to produce impulse responses of MIMO propagation channel in multi-link scenarios, and so the measurement system can be used for simultaneous measurements of dynamic multi-link MIMO channels and the data of the measurement campaigns conducted as a part of this thesis can be used for analyzing this kind of channels.

Keywords: MIMO, multi-link, measurements, interference, radiowave propagation

Tiivistelmä

TEKNILLINEN KORKEAKOULU Diplomityön tiivistelmä

Tekijä:	Jukka Koivunen		
Työn nimi:	MIMO-etenemiskanavan karakterisointi usean MIMO-linkin tapauksessa		
Päivämäärä:	10.12.2007	Sivumäärä:	67
Osasto:	Sähkö- ja tietoliikennetekniikan osasto		
Professuuri:	S-26 Radiotekniikka		
Työn valvoja:	Professori Pertti Vainikainen		
Työn ohjaaja:	DI Veli-Matti Kolmonen		

Tässä diplomityössä kehitettiin mittausjärjestelmä dynaamisen laajakaistaisen moniyhteyksisen MIMO-etenemiskanavan mittaamiseen 5.3 GHz:n taajuusalueella. Järjestelmä kykenee mittaamaan yhtaikaisesti kaksi 32x32 MIMO kanavaa, joissa maksimidoplertaajuus on 11.73 Hz. Työn puitteissa järjestettiin kaksi mittauskampanjaa joista saatua mittausdataa käytettiin järjestelmän testaamiseen ja kehittämiseen

Työn kirjallinen osuus aloitettiin kirjallisuuskatsauksella olemassaolevista MIMO-kanavamalleista ja MIMO-kanavamittauksista. Kirjallisuuskatsauksen tuloksena huomattiin ettei aiemmin ole suoritettu moniyhteyksisen MIMO-kanavan mittauksia. Myös MIMO-järjestelmän perusperiaatteisiin ja MIMO-kanavaluotaustekniikoihin tutustuttiin.

Eri mahdollisuuksia moniyhteyksisen MIMO-kanavan mittaamiseen pohdittiin ja työssä kehitettiin kahden kanavaluotaimen yhteiskäyttöön perustuva mittausjärjestelmä. Jotta järjestelmä saatiin toimimaan, täytyi TKK:n kanavaluotaimeen tehdä muutamia muutoksia.

Lopuksi työssä esitettiin mittauskampanjoiden tuloksia, joiden perusteella voidaan sanoa, että järjestelmä kykenee mittaamaan moniyhteyksisen MIMO-kanavan impulssivasteet, ja siten mittausjärjestelmää voidaan käyttää moniyhteyksisen MIMO-kanavan mittaamiseen ja työn puitteissa järjestettyjen mittauskampanjoiden tuloksia tällaisten etenemiskanavien analysointiin.

Avainsanat:	MIMO, moniyhteys, kanavamittaukset, häiriöt, radioaaltojen eteneminen

Preface

This master's thesis study was carried out in the Radio Laboratory of Helsinki University of Technology (TKK).

I would like to thank Professor Pertti Vainikainen, the supervisor of this thesis, for his advice and guidance during this thesis work.

My thesis instructor, M.Sc. (Tech.) Veli-Matti Kolmonen deserves special thanks for answering my many questions, for the invaluable help he has given me during this thesis and for giving me his excellent LaTeX template.

I would also like to thank all the people in the WILATI project. Jussi Salmi and Andreas Richter from the Signal Processing laboratory of Helsinki University of Technology deserve thanks for their help in measurement data analysis. Peter Almers and Fredrik Tufvesson from the Radio Systems Laboratory of Lund University, and Pasi Suvikunnas and Katsuyuki Haneda from the Radio Laboratory of Helsinki University of Technology I would like to thank for their help in planning and execution of the measurement campaigns. I would also like to thank Tekes for funding the project and thus this thesis in Nordite programme.

I'm grateful to all my colleagues in the Radio Laboratory for the great working atmosphere. Also the whole staff of Radio Systems Laboratory of Lund University deserve thanks for the warm welcome I got during my stay in Sweden.

Last but certainly not least, I would like to thank my family for their endless support during my studies, and the special person in my life for cheering me up during hard times.

Espoo, December 5th, 2007

Jukka Koivunen

Contents

Symbols

τ	delay
f	frequency
$\mathbf{H}$	MIMO channel matrix
$H(f)$	frequency response of the channel
$\mathbf{H}_{i,j}$	sub-matrix of the $\mathbf{H}_{MA}$ representing the MIMO link between transmitter i and receiver j
$\mathbf{H}_{MA}$	multi-link MIMO channel matrix
$H_R(f)$	frequency response of the receiver
$H_T(f)$	frequency response of the transmitter
$h(\tau)$	impulse response of the channel
$h_{i,j}$	impulse response of the channel between transmitter i and receiver j matrix
$h_R(\tau)$	impulse response of the receiver
$h_T(\tau)$	impulse response of the transmitter
T_{SL}	time difference between the TKK and LU sounders
M_R	number of RX channels in a MIMO system
M_T	number of TX channels in a MIMO system
P	number of users in a multi-link MIMO system
Q	number of access points in a multi-link MIMO system
$\mathbf{x}$	transmitted signal vector in MIMO transmission
$x(\tau)$	transmitted signal in delay domain
$X(f)$	transmitted signal vector in frequency domain
$\mathbf{y}$	received signal vector in MIMO reception
$y(\tau)$	received signal in delay domain
$Y(f)$	received signal in frequency domain

Abbreviations

AD	Analog to Digital
AGC	Automatic Gain Control
COST	European Cooperation in the Field of Scientific and Technical Research
COST 259	COST Action 259 - Wireless Flexible Personal Communications
COST 273	COST Action 273 - Towards Mobile Broadband Multimedia Networks
DA	Digital to Analog
DoA	Direction of Arrival
DoD	Direction of Departure
DUT	Device Under Test
FDTD	Finite-Difference Time-Domain
FEM	Finite Element Method
FFT	Fast Fourier Transformation
IEEE	Institute of Electrical and Electronics Engineers
IF	Intermediate Frequency
IFFT	Inverse Fast Fourier Transformation
IQ	Inphase and Quadrature-phase
LNA	Low-Noise Amplifier
LO	Local Oscillator
LOS	Line-Of-Sight
LS	Least Squares
LU	Lund University
METRA	Multi Element Transmit and Receive Antenna
MIMO	Multiple-Input Multiple-Output
MIMO-MU	MIMO Multi-User
ML	Maximum Likelihood
ML-MIMO	Multi-Link MIMO
MMSE	Minimum Mean Square Error
MoM	Method of Moments
MU-MIMO	Multi-User MIMO
NLOS	Non-Line-Of-Sight
NTNU	Norwegian University of Science and Technology
OFDM	Orthogonal Frequency-Division Multiplexing
PC	Personal Computer
PDP	Power-Delay-Profile
PLL	Phase-Locked Loop
PN	Pseudo Noise
PPS	Pulse Per Sequence
RF	Radio Frequency
RX	Receiver

RX1	Receiver number 1
RX2	Receiver number 2
SCM	Spatial Channel Model
SISO	Single-Input-Single-Output
SNR	Signal to Noise Ratio
TDL	Tapped Delay Line
TKK	Teknillinen korkeakoulu (Helsinki University of technology)
TX	Transmitter
ULA	Uniform Linear Array
VA	Virtual Array
WLAN	Wireless Local Area Network
WiMAX	Worldwide Interoperability for Microwave Access
WINNER	Wireless World Initiative New Radio

CHAPTER 1

Introduction

For developing new and more effective wireless telecommunication systems, wide knowledge of the propagation channel is needed. Channel measurements can be used in acquiring measurement data of different kind of wireless propagation channels, such as SISO (Single Input Single Output) and MIMO (Multiple Input Multiple Output) channels, indoor and outdoor channels, and channels with different cell sizes. Using parameter estimation methods, various multi-path properties of the propagating waves, such as DoD (Direction of Departure), DoA (Direction of Arrival), delay and polarization can be extracted from the measurement data, and the acquired channel information can be used in developing new channel models. Measurement data can also be used in testing existing channel models or in testing and developing new signal processing algorithms.

With constantly growing need of larger transfer capacities, MIMO technology has been extensively studied during the last ten years. This is largely because the use of MIMO can significantly increase the transfer capacity of wireless communication systems, and it would greatly enhance the spectral efficiency of wireless communication systems. During the last few years commercial WLAN (Wireless Local Area Network) products based on the pre IEEE 802.11n [1] standard draft, that utilizes MIMO technology, have been introduced by many companies and most propably in the future also other wireless networks will go towards MIMO technology.

During the last few years the wireless access networks, e.g. WLAN and WiMAX (Woldwide Interopeability for Microwave Access), have become more and more popular and this kind of networks can be found from many places, e.g. airport terminals, shopping malls or cafeterias usually have one or several networks of this kind.

As the MIMO products become more popular and more common, and as the deployment of the base stations becomes more dense, the need to understand the effects of multi-link interference becomes more important. For this purpose, measurements of MIMO propagation channel in multi-link scenarios are needed.

This work is a part of a Nordic co-operation project between TKK (Helsinki University

of Technology), LU (Lund University) and NTNU (Norwegian University of Science and Technology), in which the effect of multi-link interference, and means to reduce its effect are studied. The sounders of TKK and LU were used together to measure the multi-link channel. Within the project the measurements will be used for developing a stochastic multi-link MIMO channel model and for testing and developing new signal processing algorithms.

In this work, modifications to the TKK sounder were made. These modifications made the joint measurements with the TKK and LU sounders possible. In addition, a measurement campaign was carried out to test the measurement setup.

This thesis is organized as follows. In Chapter 2 some motivation for multi-link MIMO measurements and MIMO measurements in general is presented together with some background theory and information on MIMO systems and channel sounding of MIMO channels. In Chapter 3 the used measurement equipment is described. In Chapter 4 the measurement setup, measurement environments, measurement scenarios and needed calibration measurements are described. In chapter 5 some measurement results are shown. Chapter 6 concludes the thesis.

CHAPTER 2

MIMO Propagation Channel Measurements and Modeling

2.1 MIMO Systems

In wireless communications a MIMO system is a wireless communication system that has more than one antenna in both transmitter and receiver [2]. The use of MIMO systems enables many different benefits that can be used to increase the performance of a data transferring network [2]. These include spatial multiplexing gain, spatial diversity gain and array gain, often also referred to as beamforming gain [3].

When exploiting spatial multiplexing gain, a serial bit stream is first divided to several parallel bit streams and these parallel bit streams are then transmitted using different antennas. In reception signals are received using more than one antenna. Because of multi-path propagation, the field produced by the different transmitted signals and their multi-path components is different at every antenna at the receiver. For M_T antennas at the transmission and M_R antennas at reception at most $min\{M_T, M_R\}$ signals can be separated in the reception using signal processing.

Also spatial diversity utilizes the different fields produced by the multipath components of the signal at the different reception antennas. The difference is that now this property is used to counteract the fast fading of a single signal. Spatial diversity can also be utilized at the transmitter by transmitting the same signal from different antennas.

Array gain can be achieved by electrically steering the beam of the array to the desired direction. This way in transmission the radiated power can be directed to the desired direction and in reception the signals from the desired directions can be more efficiently received while also possible interfering signals from other directions can be suppressed or at least attenuated.

Unfortunately not all of these benefits can be achieved at the same time, full beamforming

does not allow spatial diversity or spatial multiplexing and full use of diversity excludes beamforming and spatial multiplexing. However while the use of full spatial multiplexing excludes beamforming gain, diversity can still be exploited, although the diversity is reduced [3].

Next, the signal models for different kind of MIMO systems are presented.

2.1.1 Single-User MIMO

In a single-user MIMO channel, denoted usually just as a MIMO channel, there is one transmitter with M_T antennas and one receiver with M_R antennas as shown in Figure 2.1. For the case when the transmitter transmits a signal vector $\mathbf{x}$ the signal model for the received signal vector $\mathbf{y}$ at the receiver is:

$$\mathbf{y} = \mathbf{H} * \mathbf{x} \tag{2.1}$$

where $*$ denotes convolution and the channel matrix $\mathbf{H}$ is

$$\mathbf{H} = \begin{pmatrix} h_{1,1} & h_{1,2} & \dots & h_{1,M_T} \\ h_{2,1} & h_{2,2} & \dots & h_{2,M_T} \\ h_{3,1} & h_{3,2} & \dots & h_{3,M_T} \\ \vdots & \vdots & \ddots & \vdots \\ h_{M_R,1} & h_{M_R,2} & \dots & h_{M_R,M_T} \end{pmatrix}, \tag{2.2}$$

in which $h_{i,j}$ is the channel impulse response between receiver antenna i and transmitter antenna j. It is notable that this channel matrix includes also the effect of the TX and RX antennas, and is usually referred to as MIMO channel matrix or MIMO radio channel matrix. Respectively the term MIMO propagation channel matrix is used to refer to a channel matrix which includes only the effect of the propagation channel itself and the effect of antenna configurations and other RF electronics is excluded. SU-MIMO is also the MIMO model used in current MIMO WLAN network design.

2.1.2 Multi-User MIMO

The terms MU-MIMO (Multi-User MIMO, sometimes also referred to as MIMO-MU system) are often used to mean a system, that has one base station or access point that has N antennas and multiple users that have only one antenna, and who co-operate with each other in reception and transmission [4], as shown in Figure 2.2. For a system with P users, each equipped only with one antenna, the signal model for the signal received in the access point and the model for the channel matrix, would have the same form as in (2.1) and (2.2) with $M_T = P$. MU-MIMO is an attractive technique, because the spectral efficiency of the system can be increased with only one antenna in the individual user equipment. But

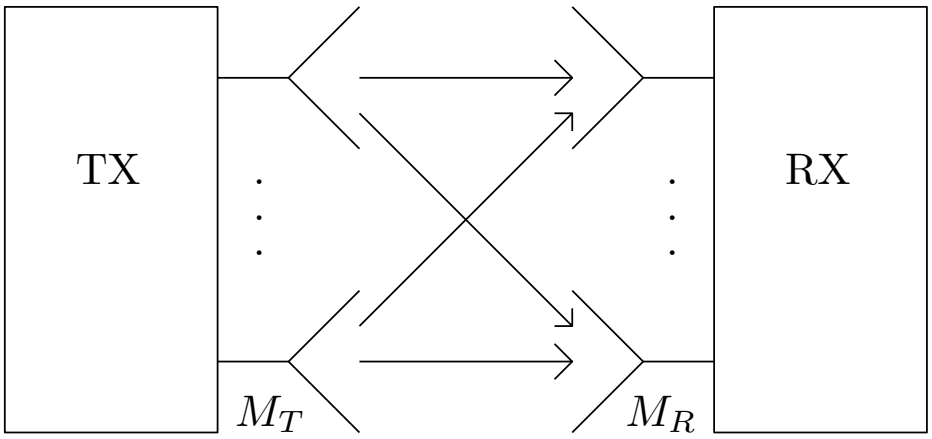

Figure 2.1: Single-User MIMO system

of course a true MIMO system still offers better transfer rates and better diversity for the individual user. Furthermore MU-MIMO technique could be utilized also with current GSM and UMTS networks, although introducing the co-operation between the users increases the complexity of the system.

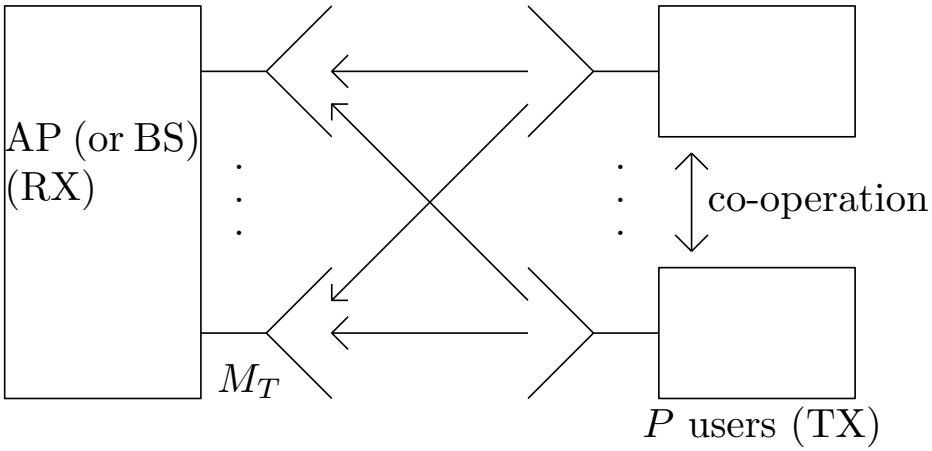

Figure 2.2: Multi-User MIMO system

2.1.3 Multi-Link MIMO

As mentioned above, the term Multi-User MIMO often means specifically a system, in which users co-operate with each other. To differentiate from this and to avoid misconceptions, in this thesis the term multi-link MIMO is used in referring to a more general scenario, in which several MIMO links interfere with each other. Users in a multi-link MIMO system might still use co-operation, but users are considered to have more than one antenna so that one individual link is always a MIMO link as shown in Figure 2.3. A typical modern WLAN environment with MIMO WLAN systems is a ML-MIMO system. For P users and Q access

points, the signal model for the signals received at the access points would be:

$$\begin{pmatrix} \mathbf{y}_1 \\ \mathbf{y}_2 \\ \vdots \\ \mathbf{y}_Q \end{pmatrix} = \mathbf{H}_{MA} * \begin{pmatrix} \mathbf{x}_1 \\ \mathbf{x}_2 \\ \vdots \\ \mathbf{x}_P \end{pmatrix}, \tag{2.3}$$

where the multi-access channel matrix $\mathbf{H}_{MA}$ is defined as

$$\mathbf{H}_{MA} = \begin{pmatrix} \mathbf{H}_{1,1} & \mathbf{H}_{1,2} & \dots & \mathbf{H}_{1,P} \\ \mathbf{H}_{2,1} & \mathbf{H}_{2,2} & \dots & \mathbf{H}_{2,P} \\ \mathbf{H}_{1,1} & \mathbf{H}_{1,2} & \dots & \mathbf{H}_{1,P} \\ \vdots & \vdots & \ddots & \vdots \\ \mathbf{H}_{Q,1} & \mathbf{H}_{Q,2} & \dots & \mathbf{H}_{Q,P} \end{pmatrix}, \tag{2.4}$$

in which $\mathbf{H}_{i,j}$ is the channel matrix between user i and access point j and is defined by (2.2).

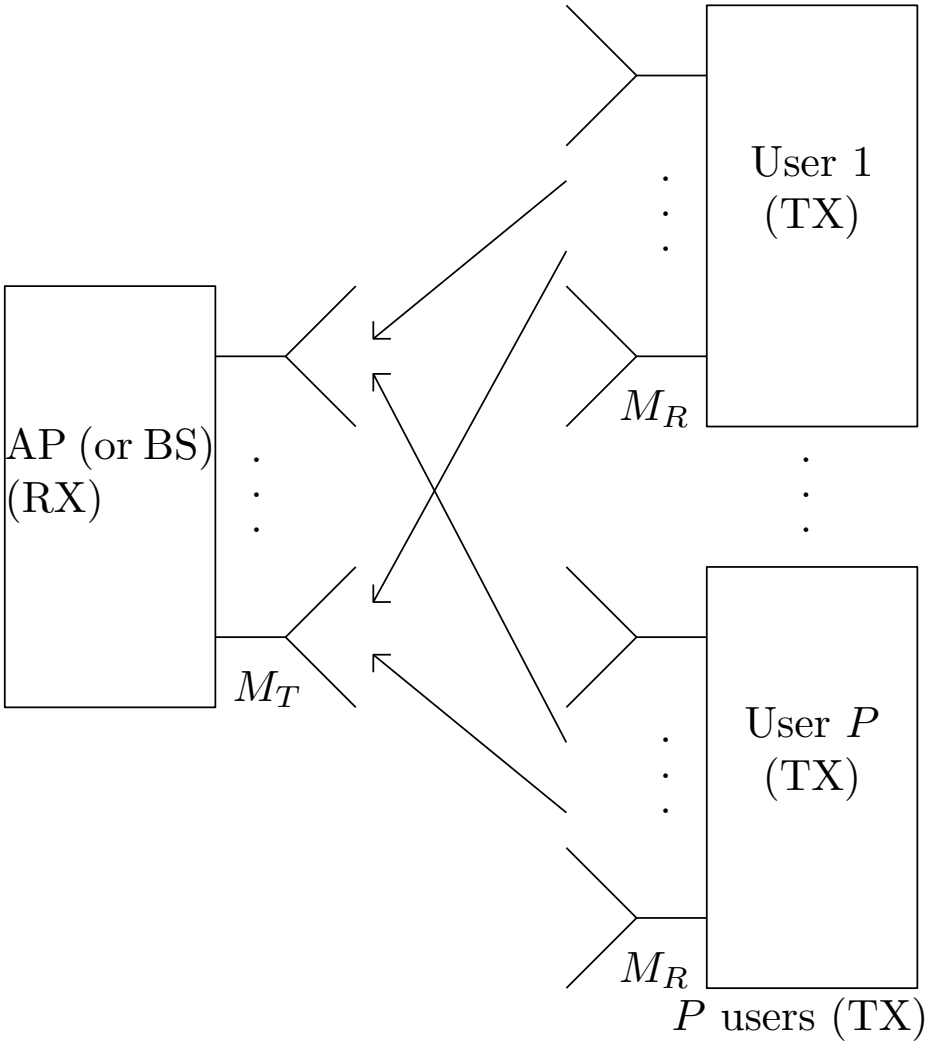

Figure 2.3: Multi-Link MIMO system

2.2 Channel Models and Channel Modeling

Channel models are an important tool in designing mobile communication systems and in network planning, because by using channel models e.g. system parameters and location of the base stations or access points can be determined so that the system or network works as close as optimal as possible, without having to do extensive measurement campaigns.

Channel models can be categorized to large scale models and small scale models, which concentrate on modeling large scale fading and small scale modeling respectively. Fading is caused by changes in the propagation environment seen by the mobile terminal, usually because of the movement of the mobile terminal. Large scale fading is fading caused by the attenuation of large objects in the environment and small scale fading fading caused by multipath propagation [5].

Previously path loss models have been, and often still are, the most common tool in network and system design [5]. In urban micro-cells and in pico-cells also directional properties of the channel are very important, especially for MIMO systems, because for example the benefits of MIMO systems mentioned in Section 2.1 are directly dependent of the directional properties of the channel. A large variety of TDL (Tapped Delay Line) models have been developed for taking in to account the delay properties of multipath channels, but to get better knowledge of the directional properties of the channel a double-directional model is needed. This kind of models can also model the dependency between DoD and DoA in addition to other channel parameters.

Channel models can also be categorized to deterministic and stochastic models, and this categorization is considered in detail here.

2.2.1 Deterministic Models

In determenistic channel modeling, specific propagation environment is studied or modeled using for example electromagnetic simulation tools, ray-tracing or channel measurements, and so a deterministic model represents some particular environment or location.

Electromagnetic simulators directly solve Maxwell's equations by using some numerical method like FEM (Finite Element Method), FDTD (Finite-Difference Time-Domain) or MoM (Method of Moments) and so they offer accurate and detailed results of all the channel properties [3]. However, due to the huge demand of computational power, the use of this kind of tools is usually limited in modeling only small structures and enviroments, such as antenna arrays and antenna structures. Electromagnetic simulations also require very detailed information of the geometrical and electromagnetic properties of modeled objects, thus further increasing the complexity of the modeling procedure significantly.

If the wavelength is sufficiently small compared to the dimensions of the obstacles in the enviroment, the electromagnetic field and the propagating wave can be modeled as rays

or beams [3]. Geometric optics theory utilizes this kind of approach. Propagation models based on geometric optics theory can be referred to as ray models. Respectively models that use rays are usually referred to as ray tracing models and models that use beams as ray or beam launching models. The use of ray models in link and network design has increased, because they are good tools especially in network-level design. Ray models can be used to reproduce the multipath propagation in the modeled environment, and this way for example the optimum location for the base stations can be determined. Advanced ray models can also model multidimensional phenomena of the multipath propagation, such as time and angle dispersion and fast fading. A fact that hinders the use of ray models is the high computation time. Also the need of accurate and extensive environment database is a significant drawback with ray models. The cost of such a database is high, and usually the available databases lack in accuracy, especially in the vertical domain. New speed-up and database reduction methods are constantly developed. Also the accuracy and reliabilty of the ray models is still somewhat uncertain; especially the estimation accuracy and reliability of other parameters than path loss, e.g. delay spread, DoA and DoD, needs development. Increasing knowledge on radio propagation and discovery of new propagation phenomena such as diffuse scattering [6, 7] results in more accurate ray models [8, 9].

Hybrid models, often also referred to as simplified models, combine the accuracy of ray models with the simplification of stochastic models. By adding statistical components to the model the need of computation time and the need for the accuracy of the enviromental database can be significantly reduced. The drawback is that the modeling capability of the model is somewhat decreased, and the output is usually limited to field strength and fading statistics only. In addition, values for the introduced statistical parameters have to be usually determined using measurements or ray tracing simulations.

Also channel measurements can be used as a deterministic channel model by using the measurement data e.g. in system simulations.

2.2.2 Stochastic Models

In stochastic channel models, sometimes also referred to as statistical channel models, the channel is modeled using statistical parameters [3]. This kind of models do not model some particular propagation enviroment. Instead the model represents some particular class of enviroments or scenarios, and the behavior of such a class is modeled statistically. However, stochastic models can usually be adjusted using a set, or sets, of input parameters to better describe the scenario and environment that is studied. The drawback of this is, that complexity of the channel model increases. The introduced parameters are usually quite abstract, and determining the values of these parameters so, that the desired scenario is represented by the model, is not always easy. Usually results of channel measurements or simulations using deterministic models are needed for determining suitable parameter values. Also a large number of these parameters is often needed for a versatile model.

The advantage of stochastic models is that the models do not require an environmental database as an input. These models are also especially good when the general functionality of some system in some kind of class of scenarios is desired. This is because with only one simulation a large number of scenarios is statistically modeled, since the statistical elements are built in to the model. Respectively, with a deterministic model, a large number of channel representations would be needed to extract statistical information.

Several different stochastic channel models exist for different purposes. Here only a few models are described shortly.

The IEEE 802.11n [1] model is a very popular channel model in WLAN design and it has been also used to some extent for designing other MIMO systems, although the model itself is designed for indoor WLAN links. The model is a part of IEEE 802.11n standard draft and a part of group of several different models [10] applicable to WLAN and MIMO WLAN design designed by IEEE TGn group.

SCM (Spatial Channel Model) [11] is a channel model that was developed as a part of 3GPP standardisation effort to be used for MIMO approaches on third-generation cellular systems. The model is designed for 2 GHz MIMO systems with bandwidth of 5MHz. In an extended version of the model, SCME [12], the frequency range of the model was extended to 5 GHz and bandwidth to 100 MHz. The extension however increased the complexity of the model.

WINNER (Wireless World Initiative New Radio) channel model [13, 14] was designed for 2 and 5 GHz MIMO systems and supports bandwidths up to 100 MHz. It is partly based on the SCME model, but unlike the SCME, it was not designed to be backwards compatible with SCM, and was instead based on measurements with 100 MHz bandwidth. A comparison of the SCM, SCME and Winner channel models is presented in [14].

COST 273 channel model [3] is a very comprehensive model for MIMO systems. It is a general channel model for MIMO systems, and it is also suitable for WLANs and fixed wireless access networks, in contrast to SCM, which is mostly concentrated on cellular networks. The downside of the generality of the COST 273 model is, that it has a large set of tuning parameters, which has caused that the model has not become very popular. Also some of the tuning parameters don't have correspondance with real world measures or phenomena, so determining suitable values for these parameters can be difficult.

SCM, COST 273 and WINNER models belong to a class of geometrical channel models, which means that they model the MIMO propagation using rays, but unlike in deterministic ray models the propagation environment is modeled with the use of statistical parameters. METRA (Multi Element Transmit and Receive Antenna) model [15], respectively, is an correlation-based channel model. This means that instead of modeling the properties of the propagation channel as geometrical channel models, correlation-based models model the properties of the MIMO matrix. This makes the model computationally efficient and simple to use, but limits the flexibility of the model, i.e. correlation-based models are designed to be used for specific antenna structures. Still, when applied correctly, the correlation-based

channel models give very similar results than ray-based channel models [16], and these models are very commonly used in system and network design.

2.2.3 MIMO Interference Models

Characterisation and modeling of the multi-link MIMO channel is not an easy task to do. The difficulties arise from the complexity of the propagation environment and the propagation channel. Already a comprehensive stochastic single-link MIMO model may demand a large set of parameters, as is the case e.g. with the COST 273 model [3]. With larger number of access points and mobile terminals the number of possible scenarios in one environment increaces. Thus in modeling and measuring the multi-link MIMO channel, it is necessary to think of the most probably occuring interference scenarios. It is also difficult to determine which parameters affect the similarity of the two interfering MIMO channels.

So far no pure double-directional multi-link models for MIMO systems exist, although some of the existing models (e.g. COST 273 and WINNER) have some ways to model MIMO interference at least to some extent. This is based on combining two single-link scenarios with a set of cross correlation parameters. At the same time because of the increasing popularity of MIMO systems and wireless networks, the need for an accurate MIMO channel model that can model the multi-link interference is growing. Thus the greatest motivation for this thesis is to get high-quality measurement data of multi-link MIMO scenarios for the development of a stochastic multi-link MIMO model.

2.3 Single Sounder MIMO Measurements

Channel measurements are an important tool in developing new channel models. Stochastic models are usually based on channel measurement data, even though some purely analytical models exist. Measurements are also used for adjusting the model parameters of deterministic models and testing the accuracy and performance of both deterministic and stochastic models. By comparing the measurements with the results produced by the model the accuracy and reliability of the model can be tested.

Traditionally, only channel path loss and channel delay characteristics have been measured. For this purpose a wideband SISO (Single-Input Single-Output) equipment can be used. But nowadays measurement of double-directional channel parameters like DoD and DoA has increased its importance. The use and research of multi-antenna systems in telecommunications has increased, and e.g. for evaluating the performance of adaptive antenna algorithms, directional information of the channel is needed. For measuring the double-directional channel characteristics, specific measurement equipment has to be used.

Previously a wide range of MIMO channel measurements have been performed. As a part of this thesis a survey was made to give an overview of previously conducted measurement

campaigns at frequency range from 2 to 5 GHz [15, 17–98]. Table 1 in Appendix 6 shows the MIMO measurements found at that frequency range listed and categorized. In the table measurements are sorted first by frequency, then by measurement bandwidth and finally by whether the measurement was static or dynamic. Here, a dynamic measurement means that either RX or TX, or both, was moved during the measurements. So measurements that have had fixed TX and RX but some movement in the environment (e.g. moving people), are labeled as static measurements in the table in contrast to usual practice. Also the measurement environment, cell size, some antenna parameters, and whether the paper presents double-directional evaluation of the measurement data (i.e.. DoA and DoD analysis), or if a parametrized channel model is derived in the paper, were collected to the table.

We can see that for a large part of the measurements, the measurement frequency coincides with WLAN frequency bands at 2.4 and 5.2 GHz. Various kind of array shapes and antenna elements have been used, although ULA (Uniform Linear Array) seems to be the most popularly used array geometry. Monopole, dipole and also different kinds of patch antennas seem all to be widely used. Both indoor and outdoor and also indoor-to-outdoor environments are represented and also different kind of cell sizes have been used. For a large part of the measurements, double-directional analysis of the data has been done, and in some of the papers, also a parametrized channel model is derived based on the measurements, even though in many papers only the non-directional channel impulse response is measured and parameters derived from that, e.g. path loss, PDP (power-delay-profile) and MIMO capacity, are analyzed. So we see that lots of MIMO channel measurements have been made, and quite extensive research and analysis of the MIMO channel has already been made in the frequency range from 2 to 5 GHz. But one area that did not appear in the papers of this survey was interference between several MIMO links. Specifically no measurements using two or more channel sounders simultaneously were found in the survey.

2.4 Interference Measurements

As seen in the previous section, various kind of MIMO measurement campaigns have been conducted and the performance of MIMO systems has been evaluated in different kind of environments, and with different kind of array and antenna structures. But still there are areas in MIMO channel modeling that need more work. One of the areas that has not been much studied upon, is the performance of MIMO systems under multi-link interference. The knowledge of the effect of interfering users and access points is important in designing effective MIMO communication systems so that they still can perform adequately well also in interference-limited environments, i.e. in environments where interfering links are present. In most cases interference is modeled as AWGN (Additive White Gaussian Noise),although sometimes also colored noise models are used, but the problem with modeling interference in a MIMO system is, that the potential interfering equipment is also a multi-antenna device, and also the interference will be affected by multi-path effects, and so it can not be modeled as AWGN. Also using colored noise for modeling the interference is difficult

for multi-link MIMO channels, because again the difficulties arise from the fact that so far there is not much information available of the nature of multi-link MIMO interference. This means that the effect of interference cannot be easily added to the models and specific channel measurements are needed for characterizing and modeling the interference-limited environment effectively and accurately.

One approach to MIMO multi-link interference measurements is to use only one channel sounder, and measure the same route several times so that the receiver (access point) will be moved to different locations for each individual run. After the measurements, these individual measurements can then be combined in a post processing process to form a channel matrix with interfering access points. The drawback of this approach is that it has to be taken care of that the channel does not change between the individual measurements. So to get more accurate results, and to be able to evaluate the accuracy of this one-sounder approach, measurements using more than one channel sounder simultaneously are needed. Additional advantage of measuring the channel simultaneously with two or more channel sounders is, that the measurement results acquired with different channel sounders can be directly compared. This way we can see how much the used sounder equipment has effect on the results and how much the results obtained with different sounders differ from each other.

2.5 Extraction of the Channel Response

For developing channel models based on the measurements, the channel parameters have to be extracted from the measurement data.

The impulse or frequency response of the channel has to be estimated from the received signal. Propagation channels are usually modeled as linear systems. Thus the received signal at the output signal of the receiver, y, can be represented as a function of delay τ with the equation:

$$y(\tau) = x(\tau) * h_T(\tau) * h(\tau) * h_R(\tau) \tag{2.5}$$

in which $*$ denotes convolution, x is the original transmission signal in time domain and h_T, h_R and h are the impulse responses of the transmitter, receiver and propagation channel respectively.

From this equation it can be seen, that in order to get the channel response from the received signal, the effect of the transmission signal and also the effects of the measurement equipment have to be removed.

Respectively in frequency domain the signal y can be expressed as:

$$Y(f) = X(f)H_T(f)H(f)H_R(f) \tag{2.6}$$

in which X is the original transmission signal in frequency domain and H_T, H_R and H are the frequency responses of the transmitter, receiver and propagation channel respectively. If the transmitted signal and the frequency responses of the measurement equipment are known, the frequency-response of the channel can be estimated for example by using ML- (Maximum Likelihood), LS- (Least Squares) or MMSE (Minimum Mean Square Error) estimation [7]. For this some calibration measurements are needed (see Section 4.2). But as the propagation channel is multidimensional, especially in MIMO case, also other channel characteristics than delay and frequency response are important for the channel modeling. These include polarization, DoA and DoD. Usually the parameters are estimated jointly using sophisticated estimators [6, 7].

For a MIMO measurement the procedure described above can be used to extract the whole system response of the MIMO channel. This means that the effect of the antenna structure and antenna element radiation patterns are included in the resulting data. However, for channel modeling usually the response of the actual propagation channel is desired, especially for geometrical modeling. If the full 3D radiation patterns of the used antennas are available (see Section 4.3 for more details), the effect of the used measurement antennas can be removed or compensated from the measurement data and as a result the so called MIMO propagation matrix can be extracted from the MIMO system matrix [6, 7].

2.6 MIMO Measurement Techniques

Different techniques can be used for measuring the MIMO channel parameters. The most straightforward method would be to use parallel transmitters and receivers. Every antenna element, or every channel, would have its own transmitter unit in the transmitter and its own receiver unit in the receiver. Thus all the channels would be measured at the same time and the measurement would be truly real-time. The problem with this method is that this kind of transmitter and receiver structures are very expensive and complicated, especially with high number of channels, which is desired.

The most popular technique is to use fast RF switches to switch the transmitter between different TX antennas and the receiver between different RX antennas. Thus every channel is measured sequentially. This is usually done so that for every TX, the whole RX channel sequence is gone through, and so every RX channel is measured before the TX channel is changed. The measurement where all the TX and RX channels are measured is called a channel snapshot. The problem with this method is that if RF switching is used both at TX and at RX, the two switches have to be carefully and accurately synchronized. Also the channel has to be considered as static during one channel snapshot. This is usually not a problem when using fast RF switches and at practical speeds of the mobile station, and so also dynamic measurements can be made. As mentioned before, the RF switch technique is the most popular MIMO measurement technique and it is also used in majority of the measurements in Table 1 in Appendix 6. Also both channel sounders used and described in

this thesis use this method for measuring the MIMO channel.

Another possibility is to use synthetic apertures or virtual arrays. In the virtual array method only one antenna is used at each end of the measurement system, and the array is constructed by measuring the channel using different antenna locations. Moving of the antennas between individual measurement points can of course be done manually, but for better accuracy and higher measurement speed usually computer-controlled mechanical scanners are used. Using virtual arrays, the full channel matrix can be measured for example using the following procedure. The location of TX antenna is kept fixed and the RX antenna is moved from point to point, and the channel is measured at every desired point. After the whole RX array has been gone through the TX antenna is moved to next measurement point and the whole RX array is gone through again the same way as before. This is repeated until all the desired TX locations have been measured. This way the whole virtual MIMO channel has been measured and we can build the MIMO channel matrix of the individually measured points as is the case also with the method that uses RF switches. The drawback with virtual arrays is that the measurement time is long, and the channel has to remain static, or one has to be able to consider it as static, for the whole measurement time. This means that only static environments can be measured, and also continuous movement of the mobile is not possible. Also measuring polarisation can be difficult, but it can be achieved by compaining virtual array method with either parallel channel or RF switching techniques. Advantages of the virtual array method are that different array shapes can be easily measured just by changing the scanner programs. In Table 1 in Appendix 6 virtual arrays are marked with (VA).

2.7 Measurement Signals

Different kind of measurement signals can be used for channel measurements and the signals can be categorized to pulse-shaped or continuous-wave signals, or to narrow- or wide-band signals. In this chapter PN-sequences (Pseudo-Noise-codes) and periodic multi-frequency signals are described in more detail, because they are used in the channel sounders used in this thesis, and some knowledge of the measurement signals is necessary for understanding the diffrencies between the two sounders. Both of these signals are wideband sequences and by modulating the carrier frequency with these signals, wideband channel measurements are possible. The sounders itself are described in more detail in Chapter 3.

PN-sequence is a binary sequence [99], which has correlation characteristics similar to noise. That means that the autocorrelation function of the signal is one, or near one when the delay τ is zero and for other values of the delay the autocorrelation function has small values. Autocorrelation function of Gaussian noise is represented in Figure 2.4(a). Respectively, autocorrelation function of the PN-sequence used in the transmitter of the TKK sounder is represented in Figure 2.4(b) together with a part of the PN-sequence itself. From these pictures we can see the similarity between the autocorrelation functions of noise and a PN-

sequence. Thus the channel impulse response can be measured directly by correlating the received signal with the used code sequence. Channel frequency response is obtained from the impulse response by using FFT(Fast Fourier Transform).

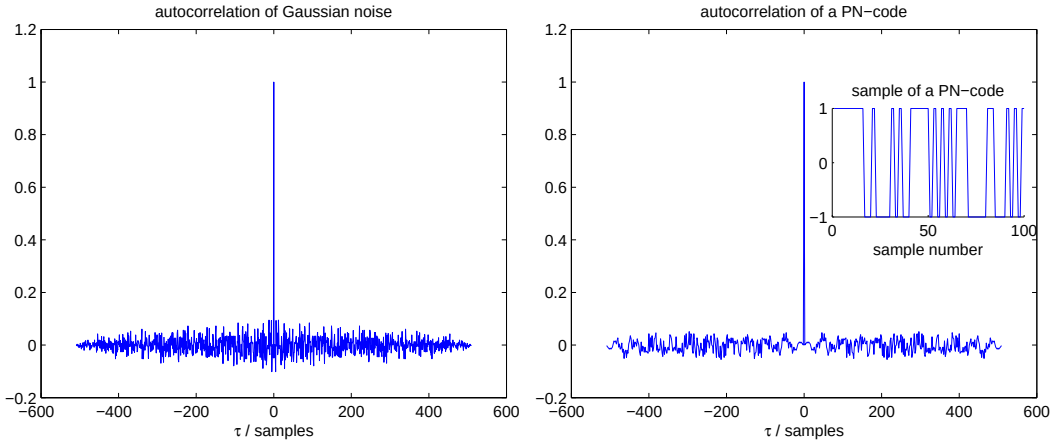

(a) autocorrelation of noise

(b) autocorrelation of a PN-code

Figure 2.4: Autocorrelation functions of gaussian noise and a PN-code

Periodic multi-frequency signal is similiar to those used in OFDM (Orthogonal Frequency Division Multiplexing). OFDM-signal is composed of several orthogonal carriers, which overlap in frequency. In data transmission complex symbols of the transmission signal are divided to different orthogonal carriers, the resulting sequence is transformed using IFFT (Inverse Fast Fourier Transform) and so an OFDM signal is obtained. In reception the signal is then decoded using FFT. The advantage of using OFDM is that instead of one signal with large bandwidth, which would be exposed to frequency selective fading, the signal is divided to very narrow sub-bands (carriers), who fade individually. For the narrow sub-bands the fading can be considered as flat fading, and the transmitter and receiver design and implementation are easier. In addition, if the channel has deep frequency-selective fading for a narrow frequency band, only the symbols that are sent with the sub-carriers in that frequency band are lost when using OFDM.

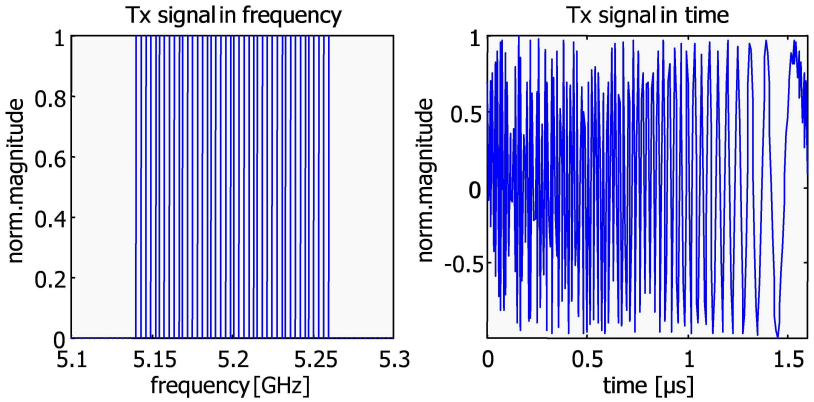

Figure 2.5: Frequency response and impulse response of the transmission code of the LU sounder

Also Periodic multi-frequency signals can be used for measuring channel responses [100]. Periodic multi-frequency signal is similar to OFDM signal, but the carriers are unmodulated. Desired frequencies and amplitudes for these subcarriers are selected, and then the signal is transformed using IFFT [7]. When the signal is DA-converted (Digital to Analog), the resulting signal resembles a frequency chirp. In Figure 2.5 a periodic multi-frequency signal used in the sounder of Lund University is represented. This kind of signal can be used for channel measurements. In the reception the channel frequency response can be measured directly and the channel impulse response is obtained by IFFT. In practice the frequency response is aquired by correlating the received signal with a reference signal. As a reference signal, usually a signal measured in a back-to-back calibration measurement is used. Back-to-back calibration measurements are described in more detail in Section 4.2. In this sense the principle of a channel sounding using periodic multi-frequency signals is very similiar to one using PN-codes, but the initial result of the measurement is the frequency response rather than the impulse response of the channel. The advantage of this kind of measurement signal is that channel frequency response can be measured at desired frequencies, and the frequency response of the signal can be selected; usually flat frequency response is desired for the measurement signal.

CHAPTER 3

Measurement Equipment

3.1 TKK Sounder

The TKK sounder is an in-house designed measurement system. It was originally built for SISO measurements at 2.145 GHz [101], but later it has been modified to work as a MIMO sounder at 2.145 GHz [102], 5.3 GHz [103, 104] and 60 GHz [105]. The sounder has also RF parts for SISO measurements at 275 MHz. The 2.145 and 5.3 GHz MIMO setups use fast RF switching and the 60 GHz MIMO setup uses mechanical scanners to create virtual arrays. In this section, the functionality of the 5.3 GHz MIMO setup is described in more detail.

The 5,3 GHz MIMO setup of the TKK sounder uses a PN-code as a transmission signal. The code has 255 chips and the chip rate at the transmitter is 60 MHz thus generating a transmission code with the length of 4.25 μs. In the receiver the signal is sampled using 120 MHz sampling rate. Sampling unit of the receiver consists of two computers enclosed to one casing. Each of the computers has its own sampling board. One of the computers acts as a master unit and samples the Q channel and the other computer acts as a slave and samples the I channel. Thus the sounder uses I-Q sampling, which means that the I and Q channels are sampled separately. The receiver of the sounder is basically a down converter and a sampling unit and all the signal processing, including the correlation of the received signal with the transmission code, is done in a post processing process using Matlab. Thus the receiver can basically be used with various kind of transmission signals, as far as the signal is in the RF-band of the receiver and can be sampled properly at the sampling rate of 120 MHz.

The synchronization of the TKK sounder is represented in Figure 3.1 [103]. During one channel snapshot N TX channels are measured. For every TX channel M RX channels and for every RX channel K TX codes are measured. In the post processing process the received signal is correlated with the upsampled version of the transmission code (consisting of 510 chips). This way, for each channel snapshot the transmission code is measured

$N*M*K$ times, and in the post processing process, desired amount of the measured impulse responses,each having 510 samples, is chosen for aquiring the channel matrix. RX and TX switching is controlled using PPS (Pulse Per Second) and trigger signals. The trigger signal is synchronized to the PPS signal and it determines the begin and the end of an individual channel snapshot. When the trigger signal goes up, RX switch starts switching. RX switch counts a predetermined number (K) of rising edges of the PPS signal before it switches the channel. In previous measurements usually $K = 2$ has been used. The RX switch cycles through the channels until the trigger signal goes down, which resets the RX switch and so sets it ready for the beginning of next channel snapshot (next rising edge of the trigger signal).

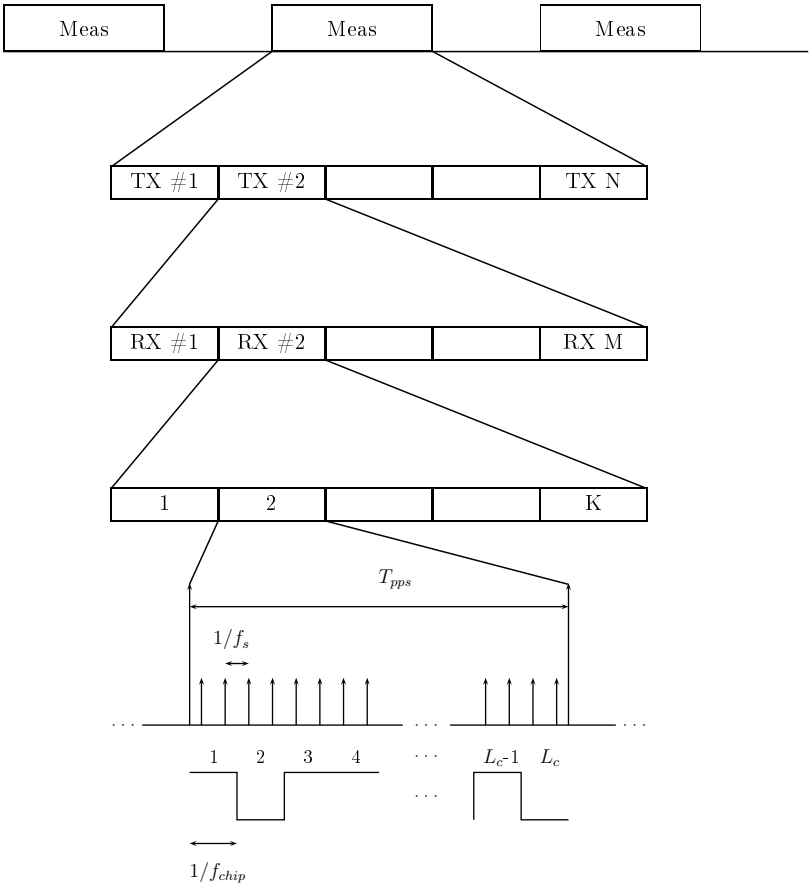

Figure 3.1: Synchronization of the TKK sounder [103]

The PPS signal is generated in the synchronization unit of the receiver, which also generates the LO signal and other RF outputs used in the receiver. The frequency of the PPS signal and the PLLs for generating the RF signals are controlled by a micro-controller.

Because during a dynamic measurement, the level of the incoming signal can vary a lot, some measures are needed to adjust the signal level before the AD-conversion. This is because, if the signal amplitude exceeds the dynamic level of the AD-converter, for every input value exceeding the maximum possible quantization level of the AD-converter, the output of the AD-converter is set to this maximum quantization level and the signal will be severely distorted or clipped as this sort of distortion is often referred to. Also if the signal

level is too low, the accuracy of the AD-conversion deteriorates because fewer quantization levels are then used. Thus an AGC (Automatic Gain Control) system is used to adjust the signal level before the AD-conversion.

The TKK sounder has two parallel subsystems, that could be used for AGC and producing the trigger signal described above. The older control unit is based on a 'heavy-duty' portable computer that is used to control the sounder when measuring with the 5 and 2 GHz setups. This portable computer has a sampling board and a DA converter board. In this older AGC system, the samples for setting the AGC values are taken from a designated AGC reference channel, using the sampling board in the portable computer, during the period when the sampling unit is not sampling. An arithmetic mean is then calculated over these samples and the acquired value is used to determine the required amount of attenuation in a LabView program. Usually an omnidirectional discone antenna has been used in the reference channel. The DA converter board of the laptop is used to generate the trigger signal.

Also a separate AGC and control unit, that can be controlled using a PC and a LabView program, exists. This system has been used with the 60 GHz measurement setup. The unit calculates the AGC values and it also generates *trig* and *monitor out* signals. Rising edge of the *trig* signal denotes the beginning of the snapshot, and the falling edge of the *monitor out* signal can be used to denote the end of the snapshot. Duty cycle of the *trig* signal can not be determined, but the length of the *monitor out* signal is adjustable. These signals can not directly be used to control the 5 GHz switches, but with a simple additional circuitry the trigger signal described above could be generated and this system could be used also with the 5 GHz setup, if some modifications are made to the LabView control program. The advantage of these modifications would be that the old control computer could be replaced with a newer one. Also the AGC differs from the older system. For time saving reasons however, it was decided to use the older system.

3.2 Sounder of Lund University

The sounder of the Lund University, from now on referred to as LU sounder, is a commercial RUSK [100] channel sounder produced by MEDAV GmbH. It uses fast RF switching and periodic multi-frequency signals. The center frequency of the sounder can be adjusted in 1 MHz steps in the frequency range 275 - 387 MHz, and in 10 MHz steps in the frequency ranges 2200 - 2700 MHz and 5150 - 5750 MHz. Also the measurement bandwidth can be adjusted in 1 MHz steps at 300 MHz range and in 10 MHz steps at 2 and 5 GHz ranges. The maximum null-to-null bandwidth in the reception is 240 MHz.

The transmitter of the LU sounder has an arbitary waveform generator unit for generating periodic multi-frequency signals. Using the waveform generator, the bandwidth of the signal and its frequency response can be adjusted. The used sampling rate at the TX is 320 MHz. In the RX the signal is sampled at a sampling rate of 640 MHz. Separate I and Q sampling

is not used but instead intermediate frequency sampling at 320 MHz is performed in the RX for recording the complex signal [100].

The synchronization of the sounder is done as represented in Figure 3.2. For every TX channel, the first RX channel (RX1) is measured at least twice, after which all the other RX channels are measured once. For every RX channel two periods of the transmission signal are received. For the duration of the first period, marked with − in the figure, the receiver does not sample and this period acts as a guard interval. During the second period,marked with +, the receiver samples and the RX channel is measured.

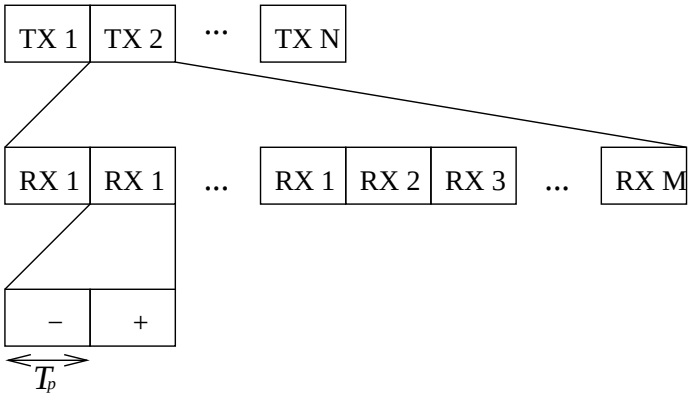

Figure 3.2: Synchronization of the LU sounder

Table 3.1: Sounder information

Parameter	LU-sounder	TKK-sounder
f_c(MHz)	5150 - 5750 (in 10 MHz intervals)	5300
BW(MHz)	10 - 240 (in 10 MHz intervals)	120
TX-code length(μs)	1.6, 3.2, 6.4, ...	4.25
Sampling rate at TX	320 MHz	60 MHz
Sampling rate at RX	640 MHz	120 MHz
RX-element switching interval (μs)	3.2, 6.4, 12.8, ...	4.25, 8.50, ...

3.3 Inter-Sounder Synchronization

The biggest challenge in the dual-link measurements presented in this thesis was to get the two sounders working together. This was especially challenging, because the two sounders used in this thesis are of different kind, i.e. the sounders are from different manufacturers and e.g. use different kind of measurement signals.

In order to receive the transmission signal of the LU sounder with the receiver of the TKK sounder correctly, the center frequencies and bandwidths of the sounders have to be the same as closely as possible. Fortunately, as we can see from Table 3.1, the center frequency

and bandwidth of the LU sounder can be tuned to match those of the TKK sounder, and with the arbitary waveform generator also the bandwidth of the transmission signal can be adjusted so that it can be measured with the sampling rate of the TKK receiver without aliasing of the signal.

One problem that can be noticed from Table 3.1 is the RX switching intervals of the sounders. This is a problem, because in order to be able to measure the transmit signal of the LU TX with the TKK RX, the length of the TKK RX switching interval has to be a multiple of the length of the TX code used at the LU TX and thus of the LU RX switching interval, which as seen from the table was not the case. Otherwise RX and TX channels start to slide regarding to each other.

Because the TKK sounder is an in-house design system, and can so be modified more easily than the LU sounder, the solution was to change the RX switching interval of the TKK sounder. This was done by changing the program of the micro-controller in the synchronization unit of the sounder. The original program was modified and the result was compiled and programmed to the micro-controller using Microchip's MPLAB development environment.

With this modification the situation shown in Figure 3.3 is achieved. RX and TX channels do not slide regarding to each other, but there exists a time difference (T_{SL}) between the channels of LU and TKK sounders. The amount of this time diference can not be known beforehand. This is because it was not possible to synchronize the TKK receiver to the LU transmitter. Fortunately the slack in itself is not a huge problem, because the value of T_{SL} will stay the same during a measurement, and also between the measurements, unless the sounders are shut down. Basically it means that it can not be known beforehand which TX channel of the LU sounder corresponds to which RX cycle of the TKK sounder, i.e. which TX is measured first. This was solved using a matched load at one TX channel and at one RX channel of the TKK sounder. By using the 'blanks', during which the received power is low, due to these so called dummy channels, it is possible to figure out the channel arragement in the post-processing process. This is described in more detail in Section 5.3

Similarly the large scale ambiguity, or problem of not knowing which snapshot of the TKK sounder corresponds to which snapshot of the LU sounder, was solved using an additional switch at the LU transmitter. The other end of the switch was connected to a matched load and the other to the transmitter. By switching the switch to the matched load for a short time in the beginning of each measurement route, a short 'blank' is generated, and by using this blank it is possible to 'synchronize' the data afterwards in a post-processing process. This additional switch was used in the first measurement, but after this it was discovered that the LU transmitter's switch that sets the RF power on and off could be used for this purpose instead. If both receivers are set to sample and the RF power is then switched on, a similiar blank is then generated to the beginning of the measurement. The procedure is explained in more detail in Section 5.4

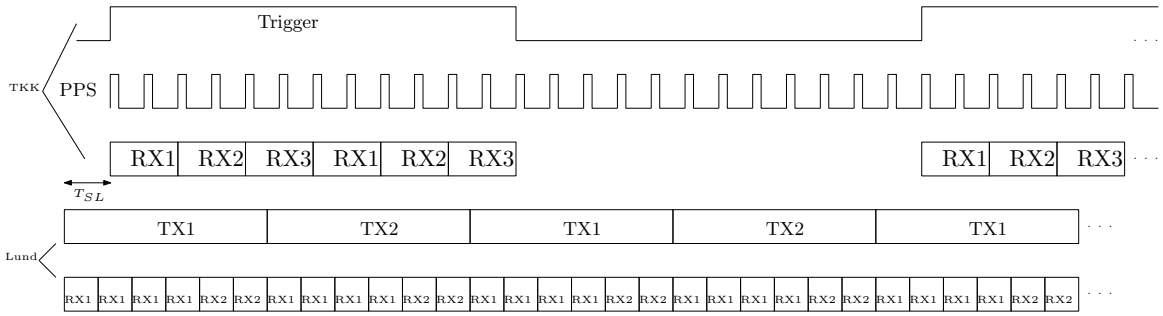

Figure 3.3: Synchronization between Lund and TKK sounders

3.4 Antennas

In the measurements described in this thesis, three antenna groups [1] with nearly isotropical radiation patterns were used. These include two spherical antenna groups by TKK [103,104] and a cylindrical antenna group by LU [107]. The spherical TKK antenna group with 45° slanted polarizations is used at the TX together with the high power transmission switch of Lund university. The spherical TKK antenna group with horizontal and vertical polarisations is used at the RX of the TKK sounder with a TKK RX switch. At the RX of the LU sounder the cylindrical antenna group with horizontal and vertical polarisations is used together with the LU RX switch. The used antennas are shown together with the switches in Figure 3.4. The transmitter antenna together with the high power transmission switch is on the left, the antenna-switch combination used at the TKK receiver is in the middle and the antenna-switch combination used at the LU receiver is on the right. The used LU transmitter switch can withstand 10 W of input RF power. All of the used switches have 32 channels.

All the antenna groups use dual polarized probe-fed rectangular stacked microstrip patch antennas as antenna elements. The specifications of the elements are represented in Table 3.2.

3.4.1 Antenna Group Geometries

The cylindrical antenna group consists of 4 rings of dual polarized antenna elements, and so the antenna has 64 dual polarized antenna elements in total. From these 16 elements were used. Eight elements of each of the two middle rows were selected so that the elements of these two rows are interleaved.

Both of the used spherical antennas have 21 dual polarized elements, of which 15 were used for these measurements. In addition to these an omnidirectional discone antenna and a

[1] In this thesis, the term antenna group is used for general antenna configurations that do not fulfill the condition of an antenna array, where the array factor and the element pattern are separable [104, 106].

Figure 3.4: The used antennas with the switches

dummy channel were used both at the transmitter and at the TKK receiver.

Table 3.2: Antenna Element Information

Parameter	cylindrical antenna group	Spherical antenna group
Frequency range	5.06 - 5.9 GHz	5.2-5.4 GHz
Return loss	< 10 dB	< 10 dB
Polarization discrimination	15 dB	18 dB
Gain	5.1 dB	7 dB
Isolation (d = $\lambda/2$)	9.2 dB	15 dB
Polarization	H/V	H/V or 45° slanted

CHAPTER 4

Measurements

4.1 General measurement setup

The best possible setup for the channel sounder measurements with two channel sounders would of course be to use both channel sounder systems as a whole to acquire a full multi-link MIMO system with two transmitters and two receivers. This kind of setup is represented in Figure 4.1. The advantage of this kind of setup would be that the whole multi-link MIMO matrix could be measured. This setup would however require using transmission codes that are orthogonal compared to each other so that the two signals can be separated from each other in the receivers. Unfortunately the TKK code generator uses a PN code and it can not be synchronized with the LU transmitter, which means that a code that would be orthogonal to such a signal at every time instance does not exist. Also the LU RX was not able to receive the TKK TX signal without modifications.

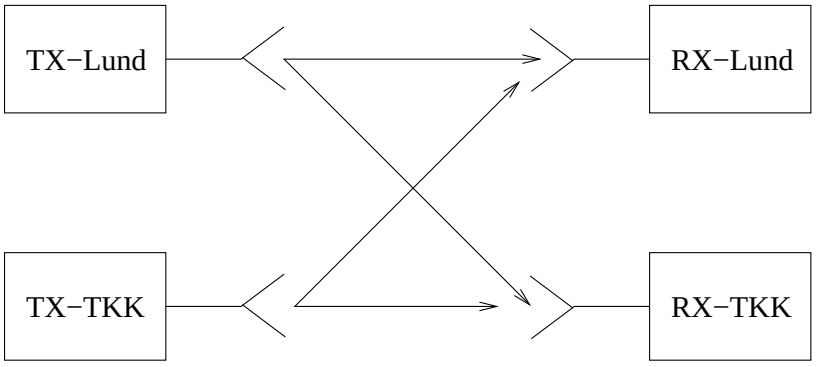

Figure 4.1: Full two-link measurement setup

For this reason it was decided to use a setup represented in Figure 4.2. In this setup, the LU transmitter transmits a signal that is received by LU and TKK receivers. This way a multi-link MIMO system either with one access point and two mobile stations or with two access points and one mobile station could be emulated, if the channel is assumed to be recirocal as usually is the case. It was decided to use mainly the latter approach, where

transmitter represents a mobile station and the two receivers represent two separate access points, because it was considered to be the situation occurring more often in real systems. This approach makes also the design of the measurement routes and measuring a lot easier, because there is only one moving mobile station. For two moving mobile stations it would be difficult to design the measurement routes so that they represent real situations, and a large number of measurements would be needed to model statistically how the movement of two moving mobile stations in regard to each other affects the channel.

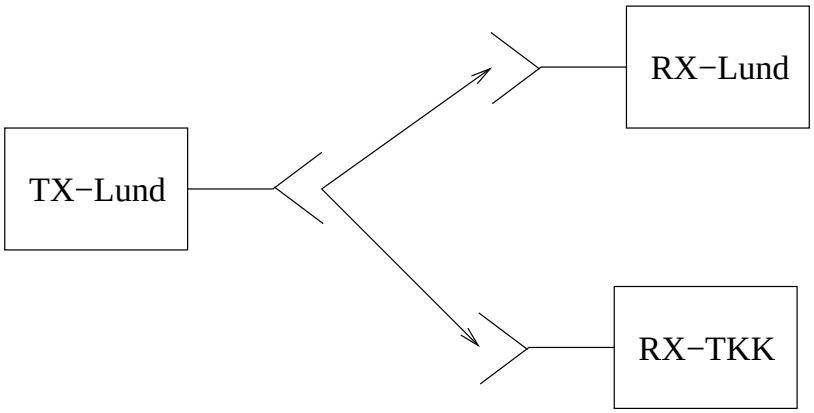

Figure 4.2: Used measurement setup

An alternative approach would have been to use the setup represented in Figure 4.3. In this setup, the two full measurement systems are used and the transmitted signal is switched between the two transmitters. So each receiver samples continuously, while the transmitters are switched, so each transmitter transmits in turns. This means that each receiver will measure both, signal from its own transmitter and signal from the other transmitter. The parts measured while the other transmitter was transmitting have to be discarded in the post processing process, which means that only at maximum only about a half of the measured data can be utilized. The advantage of this kind of setup would have been that no modifications to the sounder equipment itself would have been needed.

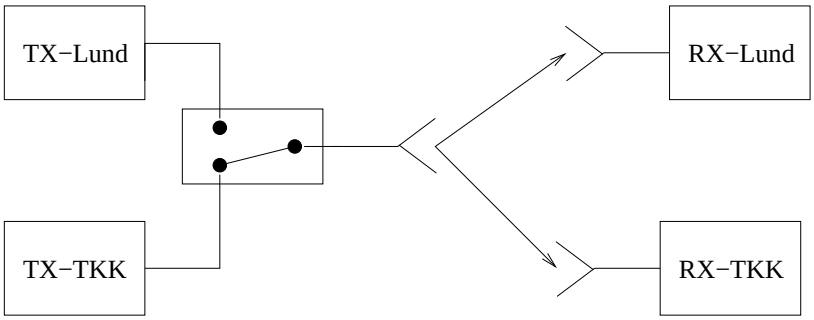

Figure 4.3: Alternative measurement setup

4.2 Back-to-Back Calibration Measurements

A back-to-back calibration measurement is a measurement, in which the output of the TX is connected via a cable, which was used here, or other transmission channel that can be considered as ideal or nearly ideal, to the input of the RX. The purpose of this kind of measurement is to acquire a reference signal to be used as a reference in the acquisition of the frequency response. Using this kind of reference in the correlation instead of the transmitted code has the advantage that when using a measured reference, the effect of the frequency response of the transmitter and receiver units, is compensated. Of cource the frequency response of the additional cabling and attenuation used in the back-to-back measurement needs to be measured and compensated. When the use of back-to-back calibrations is combined with the data of wideband antenna calibrations, the effect of measurement hardware can be removed from the measured data and so the acquired channel response will be the response of the channel itself, not a combined response of the channel and the measurement equipment. A separate back-to-back measurement is needed for both TX-RX pairs.

For the dual-link measurements done in this thesis also a specific dual-link back-to-back measurement is needed. The set-up for this measurement is represented in Figure 4.4. The output of the TX was connected to the input of each of the receivers by using a power splitter to split the signal. The adjustable attenuator is used to adjust the signal level in 10 dB steps. The purpose of this kind of measurement is to measure the difference in dynamic levels between the two receivers. Using this information, the difference in received power can be compensated in the post-processing.

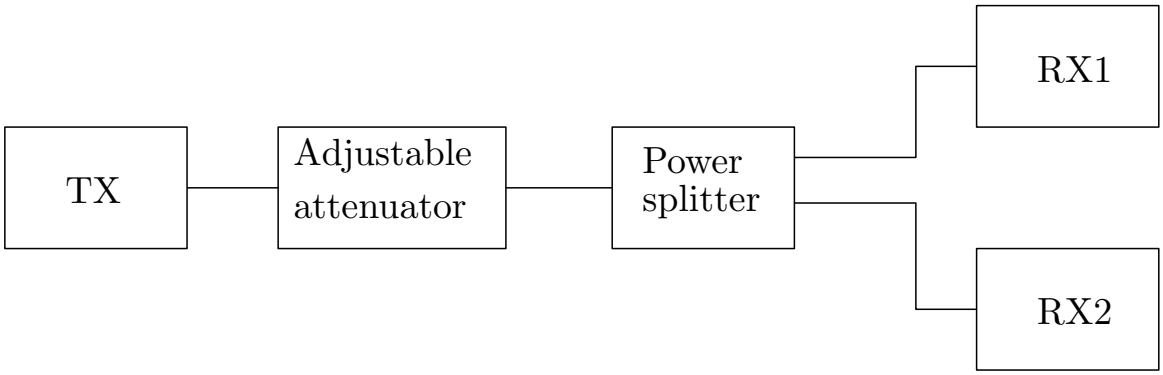

Figure 4.4: Dual-link back-to-back calibration measurement setup

4.3 Antenna Calibrations

The purpose of antenna calibrations is to measure the full 3D radiation pattern of the used measurement antennas. Results of the calibrations can then be used to remove the effect of the non-idealities of the antenna-switch combinations from the measurement results.

Antenna calibrations were done in Lund at Sony Ericsson with a Satimo Stargate 64 an-

tenna measurement system. This is a near-field measurement system, which means that it measures and stores measurement results as near-field measurements, from which the far-field results can be calculated in a post-processing process using a specific near-field to far-field transformation based on spherical wave expansion [108]. The sounders were not used in the measurements. Instead, the signal generators of the measurement chamber were used as signal sources and specific control circuits were used in changing the channels of the switches. The measurement protocol was such that first the DUT (Device Under Test) was rotated to a specific angular position and then all the frequency points were measured sequentally. In total 21 frequency points in the frequency range of 5180-5420 MHz with 12 MHz steps were used. It was noticed that after each rotation the antenna was shaking a bit. This was most likely because of the substantial weight of the antenna-switch combination. Unfotunately there was no possibility to support the antenna-switch combintaion better so that the shaking would have been damped, and so the solution was to measure the first frequency point three times for every angular position to reduce the effect of the shaking of the antenna. During the measurement of these two additional frequency points in the beginning of each angular position the shaking of the antenna was damped signifigantly and so the effect of the shaking was sustantially reduced.

The LU RX switch has an inbuild LNA (Low Noise Amplifier). This was a problem because in the measurement chamber the DUT was set to be transmitting, and there was no option to change this. Fortunately there was an option to bypass the LNA of the switch by connecting two ports outside the switch together. This was done, and the antenna-switch combination could be used in transmission. The response of the LNA was measured separately with a VNA and the result was combined together with the calibration results. The two other antenna-switch combinations were not calibrated at this time, because of time-issues and because of a hardware-issue in the LU TX-switch.

4.4 First Measurement Campaign

The first measurement campaign was carried out in the premises of Lund University in two different kind of propagation environments. The first measurement environment in this campaign was the radio systems laboratory wing at the E-building and it represents a typical office environment. A floorplan of the wing is represented in Figure 4.7 and a photograph of the main corridor in this wing is represented in Figure 4.5. The floorplan also shows one of the measurement scenarios in this environment. In the map the LU receiver is labeled as RX1 and TKK receiver as RX2. As seen from the figure, the receivers were located in rooms for these NLOS measurements. In one measurement TX was moved from the front of room 2372 to the front of room 2374. In the other measurement TX was moved randomly in a small area marked with a purple spot in the figure. In another scenario receivers were positioned in different ends of the corridor.

The second measurement environment was the entrance hall of the E-building of Lund

Figure 4.5: The measurement equipment in positions for a short range LOS measurement in the Radio Systems Laboratory corridor. The TKK RX is at the right in the front, The LU RX can be seen at the end of the corridor, and the LU TX is located in the middle of these two.

University. The floorplan of the entrance hall is represented in Figure 4.10 and a photograph of the hall in shown in Figure 4.6. The entrance hall is a long hall with nearby corridors and lecture halls and it can represent e.g. an airport terminal, or a part of a shopping mall. Figure 4.8 shows how the sounders were positioned in one of the static LOS measurement scenarios in the entrance hall. At first the LU receiver was positioned to the point A and TKK receiver to the point B. A few measurements were made and the positions of the receivers were switched and after this, new measurements were made. Because the channel did not change between the switch of measurement positions, these measurements can be used to determine how much the results obtained with different receivers differ from each other. Figure 4.9 shows a dynamic LOS scenario, in which the TX was moved between the two RXs in the entrance hall.

Also one particularly interesting measurement was made in the hall and in the nearby corridor. This measurement scenario is presented in Figure 4.10. In this measurement TX was moved from next to RX1 to next to RX2 around the corner, and this way it moves from LOS of one receiver to the LOS of the other receiver. This type of measurement scenario represents a real life application with two WLAN access points, one in the entrance hall and one in the neighboring corridor.

Figure 4.6: The transmitter in the entrance hall

In all of the measurements in the first measurement campaign the time between individual channel snapshots was 42.6ms and so the snapshot measurement frequency was 23.47 Hz and the maximum doppler frequency that could be measured was 11.73 Hz

4.5 Other Measurement Campaigns

After the first measurement campaign, a data-clipping issue was found from the measurement data and the issue greately hindered the use of the data. Detailed description of the issue and possible solutions are presented in Section 5.5. Thus a second measurement campaign was conducted in the premises of Lund University during this thesis. The purpose of this campaign was to verify that the solution for the data-clipping issue was successfull, and also to measure again some of the most interesting scenarios of the first campaign. The same measurement environments, and also some of the same measurement routes or scenarios, as in the first measurement campaign were used in addition to some new scenarios. Also the measurement setup was the same, except due to a hardware failure in the LU TX switch only half of the channels of the switch were functional, and so only 16 TX channels could be used. Hence only 7 dual polarized elements of the TX antenna group were used together with a discone antenna and a dummy channel for the measurements of this campaign. Due

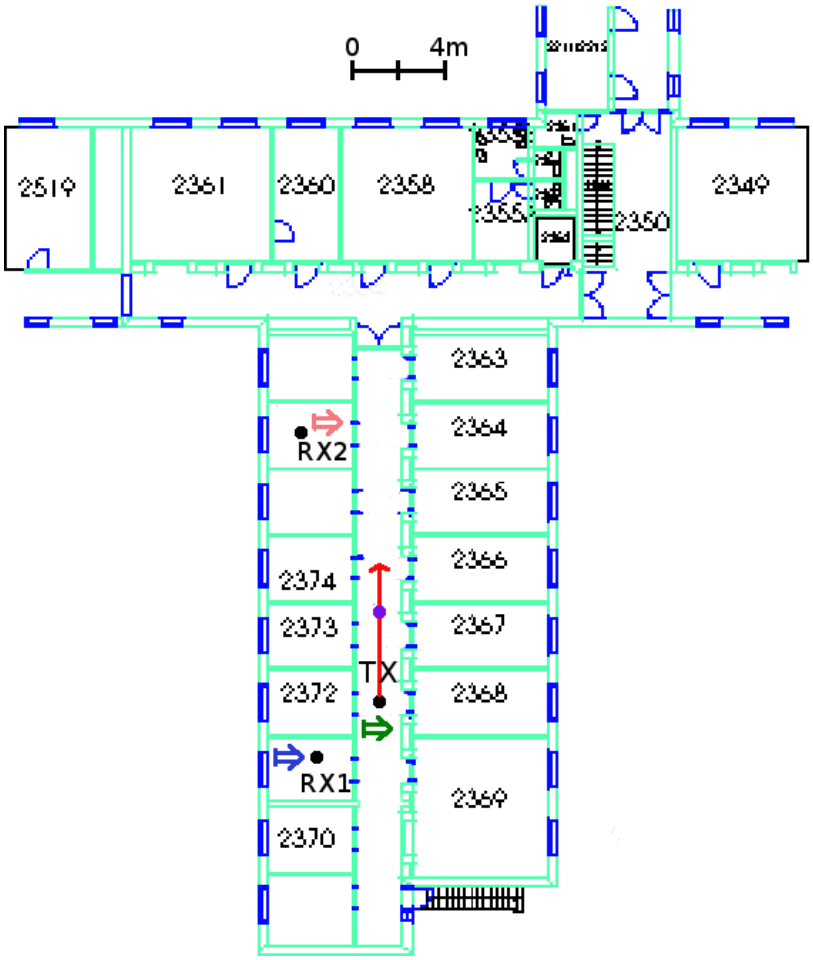

Figure 4.7: Measurement map of a NLOS measurement scenario in the Radio Systems Laboratory wing

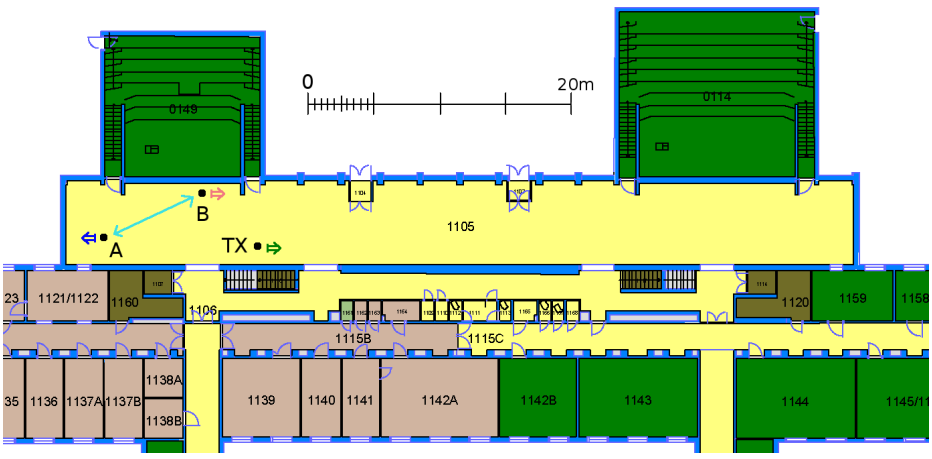

Figure 4.8: Measurement map of a static LOS measurement scenario in the entrance hall

to the smaller number of TX elements, it was decided that the antennas were not calibrated for this campaign, because the resulting TX antenna structure was considered to be insufficient for achieving good DoD estimation. Thus in this measurement campaign the focus was in measurements that could be used for algorithm testing and development.

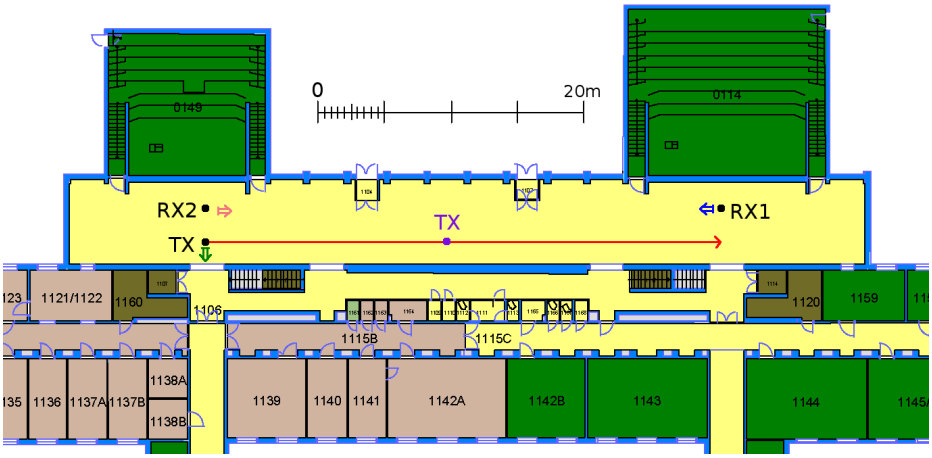

Figure 4.9: Measurement map of a dynamic LOS measurement scenario in the entrance hall

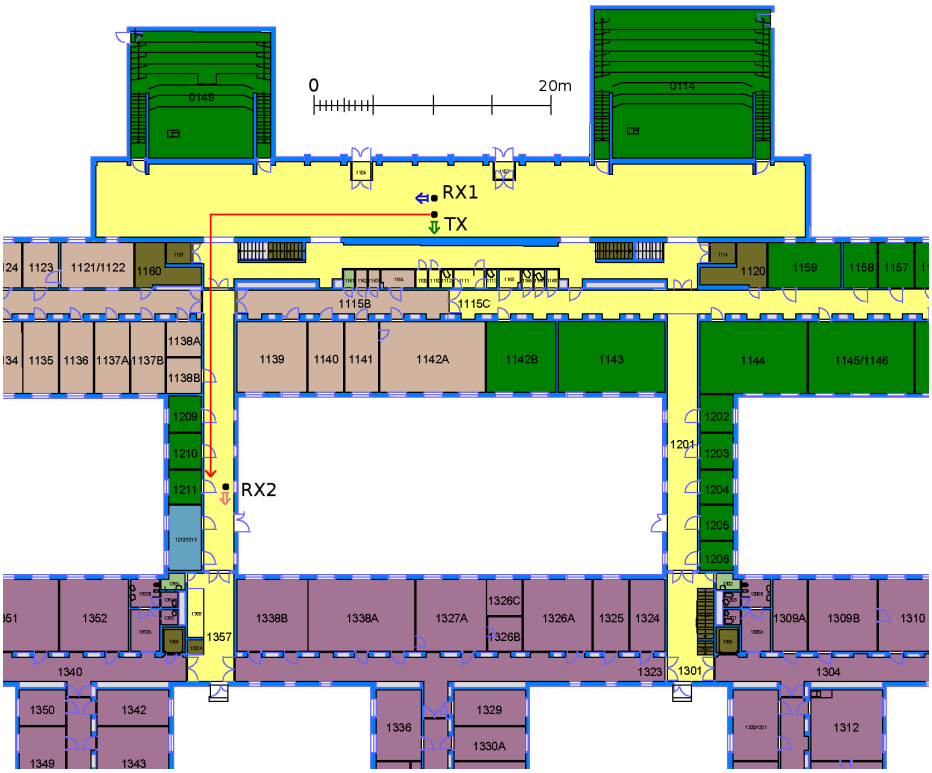

Figure 4.10: Measurement map of a corridor measurement scenario in the entrance hall

In addition to these two measurement campaigns conducted in the premises of the Lund University, also a third measurement campaign was concluded during the finalization of this thesis, this time in the premises of TKK (Helsinki University of Technology). This third measurement campaign was conducted in an shopping-mall like environment in a Computer Science building of TKK. For this third measurement campaign, all the antenna groups were now calibrated and so the measurement results can be used for geometric modeling purposes.

For the measurement of the second and third measurement campaign, the same maximum doppler setting as in the first measurement campaign was used.

CHAPTER 5

Results and Data Post-Processing

5.1 Channel Matrix

The used measurement setup, represented in Figure 4.2, has one transmitter and two receivers. Both the transmitter and each of the receivers have 32 channels. Thus the acquired multi-link channel matrix has the form:

$$\mathbf{H}_{MA} = \begin{pmatrix} \mathbf{H}_{1,1} \\ \mathbf{H}_{2,1} \end{pmatrix}, \tag{5.1}$$

in which $\mathbf{H}_{1,1}$ is the channel matrix of the channel between the transmitter and receiver number one, and respectively $\mathbf{H}_{2,1}$ is the channel matrix of the channel between the transmitter and receiver number two. If also the reference channels with discone antennas and the dummy channels are included, these individual channel matrices are both defined by Equation (2.2) with $M_T = M_R = 32$. Usually in the actual usage of the data the dummy and reference channels are excluded, and then $\mathbf{H}_{1,1}$ will have $M_T = 30$ and $M_R = 32$ and $\mathbf{H}_{2,1}$ will have $M_T = M_R = 30$.

5.2 Hold of the Synchronization

Possibly the most critical aspect for the success of the measurements was that the partial synchronization between LU and TKK sounders, described in Section 3.3, holds. That is because, if the synchronization does not hold, TKK RX channels starts to slide in regard to TX channels, and the measurement data could not be utilized. Before the actual measurement campaigns the synchronization hold was verified by doing back-to-back calibration measurements, where the output of the TX was connected via a cable to the input of the

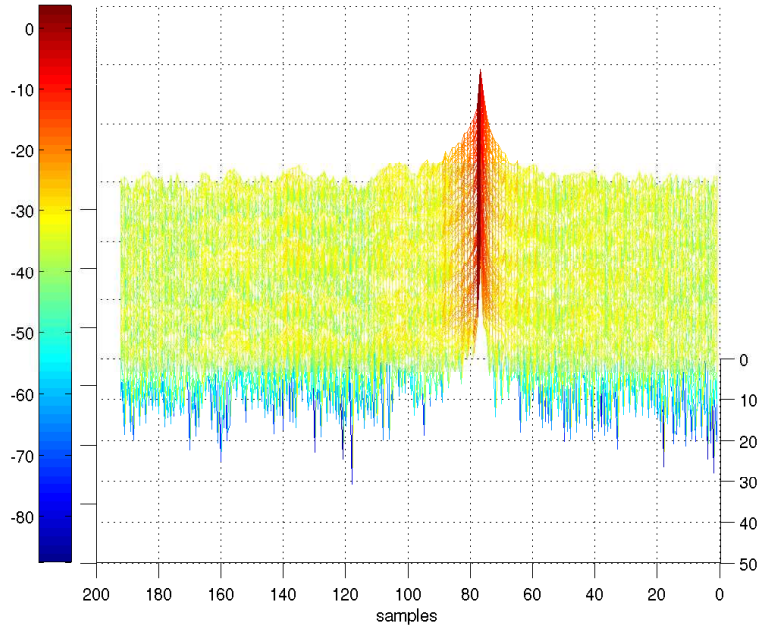

Figure 5.1: The first impulse response of every snapshot in a back-to-back measurement

TKK RX as described in Section 4.2. The hold of the synchronization can be examined from back-to-back-measurements by first correlating the measurement data with a reference signal. This way an impulse response is acquired. In a back-to-back measurement, the peak in the impulse response should stay in the same location in time, or in samples, for the whole measurement, because the channel is static. First impulse response of every snapshot of the correlated back-to-back measurement is represented in Figure 5.1. It can be seen that the synchronization holds firmly for the whole measurement.

The hold of the synchronization can also be verified using data from the actual measurements. In Figure 5.2 a section of the I-channel raw data, i.e. the sampled data of the I-channel sampling board before any post processing, is shown of a measurement made in the entrance hall with the full measurement setup. In this measurement TX moved from next to RX2 (TKK RX) to next to RX1 (LU RX) as shown in Figure 4.9. In Figure 5.2 we can see a part, in which the amplitude of the signal is very low for each snapshot (between samples 10000 and 25000. This is due to the dummy channel used in the transmitter. Thus if the location of this dip in signal amplitude in samples is the same for all the snapshots, for a static measurement, the synchronization holds. From the figure we can see that the synchronization seems to hold quite well. A closer look reveals that there exists approximately a 10 sample difference between the first and the last snapshot. However from the raw data the situation can not be easily seen. The fact how accurately the synchronization holds is better seen by examining the impulse responses in the same way than above with the back-to-back measurement. During a static LOS (line of sight) measurement the location of the peak in the impulse response, should stay the same in time, but of course if the channel is not quite static the location of the peak may still change between snapshots even though the synchronization holds. In the measurement under examination, the TX was moving, and

so from Figure 5.3 it can be seen that the location of the peak in impulse response changes. A closer examination reveals that the difference between the first and the last snapshot is 13 samples. With a sampling rate of 120 MHz this translates to a delay difference of 108.3 ns, which corresponds to a distance of 32.5 m between the starting and ending point of the TX movement. This agrees well with the measurement scenario, and so the synchronization hols also in real dynamic measurement scenarios. So in total it can be said, that the modifications of the TKK receiver were successful and the partial synchronization between the two sounders holds and works as was planned.

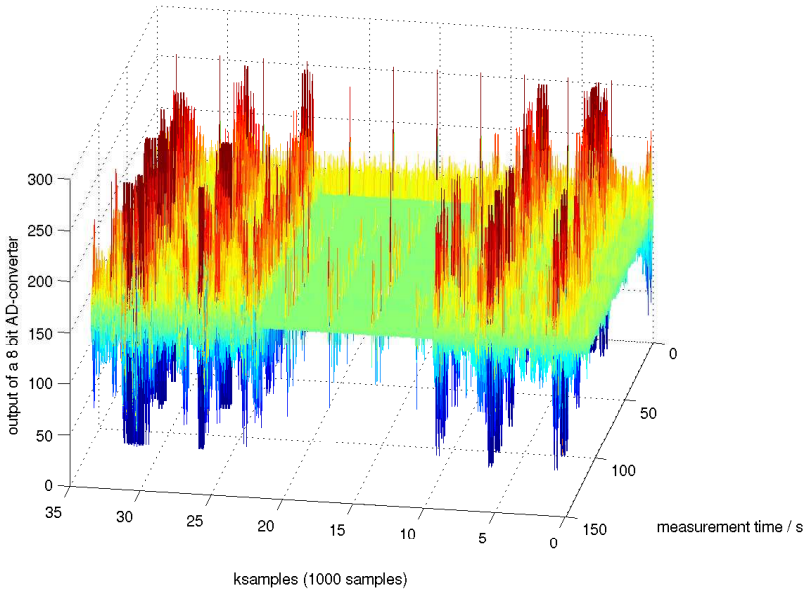

Figure 5.2: Section of I-channel raw-data of every snapshot showing the TX dummy channel in a dynamic measurement with the full measurement setup

5.3 Reordering Process of the Data Measured with TKK RX

Because of the partial synchronization between the two sounders, described in Section 3.3, the slack T_{SL} shown in Figure 3.3 can not be known beforehand. This means that the data measured with TKK receiver has to be reordered and pre-processed before it can be utilized. For this reason the impulse response represented in Figure 5.3 is not the final impulse response of the channel. In the reordering process, first the dummy TX channel, the second TX channel in these measurements, is searched from the snapshot. From the beginning of this dummy channel the switching instances of other TX channels can be calculated and TX channels can be ordered so that this dummy channel is in the same place of the snapshot as in the measurement. Respectively, the position of the TX switching moment in regard to the RX channels is identified using the RX dummy channel. The switching sequence of the TKK RX is fully known because the sampling always starts from the first RX channel, as indicated in Figure 3.3. This way the location of the switching instance of the dummy channel in samples can be determined, and the RX channels can

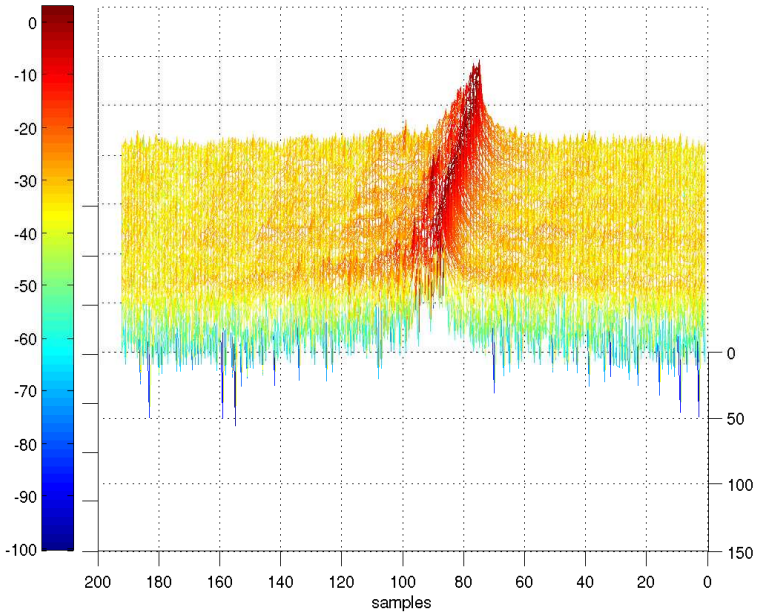

Figure 5.3: The first impulse response of every snapshot in a dynamic measurement with full measurement setup

be ordered in to the correct order for each TX channel. The correct ordering of the RX channels can then be verified by looking for the position of the RX dummy channel from the reordered data. For these measurements the RX dummy channel was the second RX channel. After this, for each RX channel, a section of the data is selected from the two received TX code sequences so that a whole TX code sequence is included, and that the TX and RX channel switching instances are not included.

It was decided that no reordered raw data is stored. Instead an index vector, which contains the information of which samples to read and in which order to achieve the correct reordering, was saved for each measurement. This way a large amount of hard-disk space is saved and from the same data either the raw data samples or reordered data, which ever is needed, can be read, although data reading is significantly slower. These index vectors were made using a specific Matlab function.

Figure 5.4 shows the I-channel raw data of one whole TX channel and a part of the TX dummy channel. The beginning of the TX dummy channel is marked with a green vertical line, and the switching instances of the TKK RX with red vertical lines. From the figure the RX dummy channel is clearly seen as a short section with low signal level beginning from the sample index $2.46 * 10^5$. Respectively the TX dummy channel is seen as a longer section with low signal levelat the end of the figure. It can be noticed that the TX switching interval, the green line, does not align exactly with the RX switching interval in this particular measurement. This is due to lack of full synchronisation, described more in Section 3.3. The reordered version of the same data section is represented in Figure 5.5. From this it can be seen, that the length of the reordered data in samples is only half of that of the raw data. This is because only one code sequence of the measured two is utilized for each RX

channel. Also notable is, that a section that is in the end of the TX channel in Figure, so the section before the TX dummy channel containing the RX dummy channel, 5.4, is now in the beginning of Figure 5.5. So, now the RX dummy channel is the second RX channel as it should be. The data contains now one full transmission code sequence per each RX channel and the RX channels are now in the correct order for each TX channel.

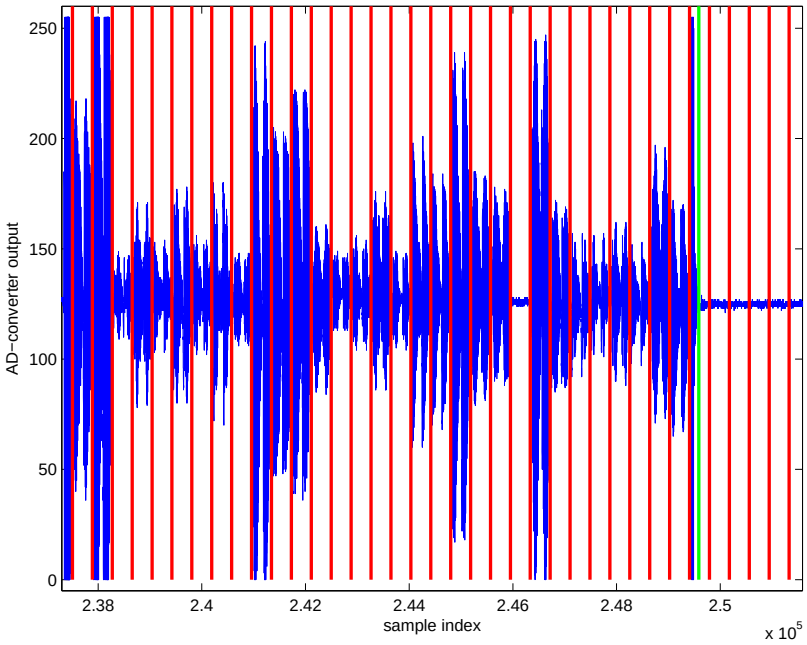

Figure 5.4: A section of raw data showing one measured TX channel and a part of the TX dummy channel

5.4 Snapshot Synchronization between the TKK and LU Sounders

After the data reordering has been done for the TKK data, the TKK data is in correct channel order and it can be utilized. There is however still one post-processing process that needs to be done, before the data of the two sounders can be used together. Because the two sounders are not fully synchronized, the sounders do not start measuring at the same time. Thus, the synchronization of the snapshots between the TKK and LU sounder has to be done in the post-processing. In the measurements the TX power is switched on shortly after the sampling is switched on at both receivers. Hence the MIMO snapshots of the TKK and LU sounders can be synchronized by using the snapshots, during which the power is switched on as a reference, as far as the SNR at the receivers is good enough at the time when the power is switched on.

In Figures 5.6 and 5.7 the average power of each snapshot is shown for the 100 first snapshots, for the same measurement and for TKK and LU sounder data, respectively. From the figures the snapshots during which the received power starts to rise can be clearly seen. So in this

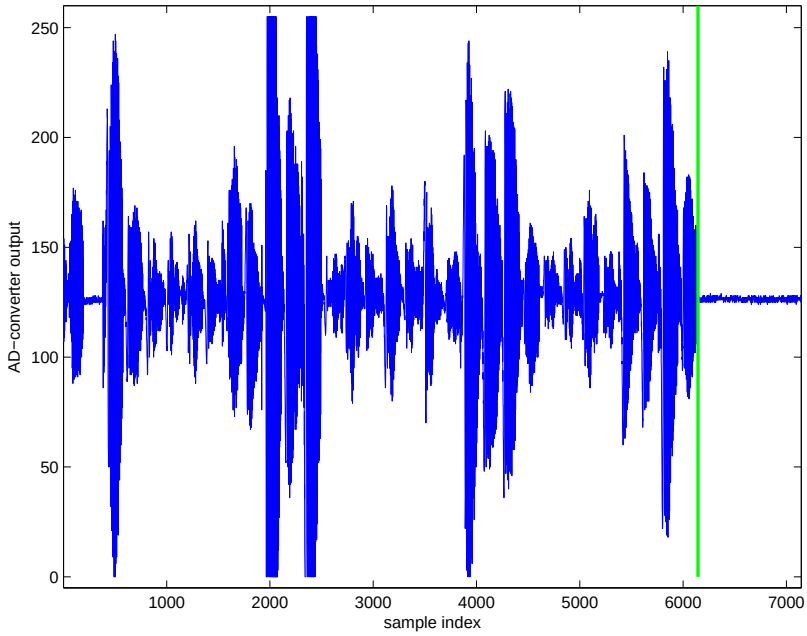

Figure 5.5: The same section of data as in Figure 5.4 after the reordering process

measurement the TX is switched on while the TKK RX is measuring the snapshot number 44 and LU RX the snapshot number 80.

5.5 Data Clipping

During the post processing of the data from the first measurement campaign, it was noticed that clipping of the signal appears in the data measured with the TKK receiver. Some clipping can be seen from Figures 5.4 and 5.5. Because the AD-converters of the TKK RX have 8 bits, the largest possible output value is 255 and the smallest is 0 and so for clipped channels the signal is limited to these values. It seems that in the data of Figure 5.4 four transmission code sequences and in the data of Figure 5.5 two transmission code sequences have been clipped. Thus for the particular TX channel shown in the figures, two RX channels have been clipped during the snapshot. Data of these two clipped channels and the effect of clipping are better seen from Figure 5.8, which shows a closer look of the clipped channels of reordered I-channel raw data in Figure 5.5.

The reason for this clipping is that the attenuation value in the AGC system has been too low and so the input level to the AD converter boards has been too high. Of course some clipping may always happen, because the range of the AGC is limited, but it was noticed that in this case the clipping is present in all of the measurements of the first measurement campaign and that it occurs quite frequently during the measurements. This limits greatly the utilization of the measurement data, because the clipping corrupts the channels with the largest received signal power, and so with the best SNR (Signal to Noise Ratio). These are also the most interesting channels, because for example in parameter estimation better

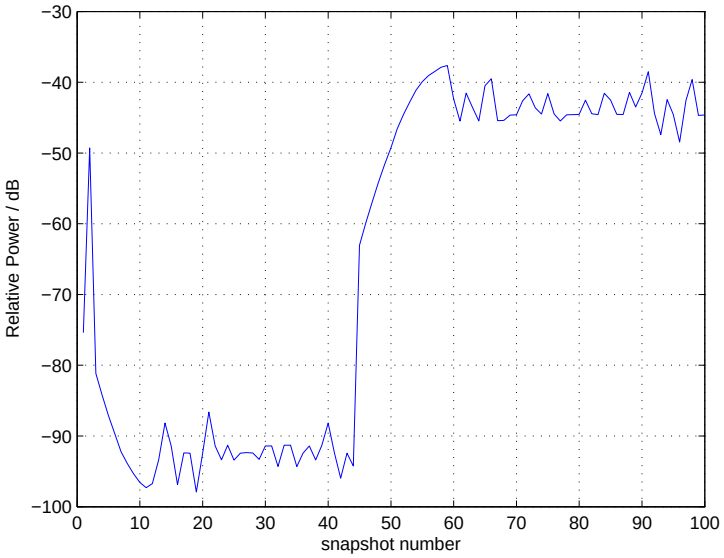

Figure 5.6: Average power of each snapshot from the beginning of a measurement, TKK data

estimates are achieved with better SNR.

Some reasons for the clipping can be seen from Figure 5.5. The TKK AGC system takes the samples for determining the proper AGC channel from one single RX channel which is the first RX channel in these measurements. From Figure 5.5 it can be noticed that the signal level in this first RX channel is clearly lower than in some of the other RX channels. Thus the AGC is set to too low a value, and the strongest RX channels will probably be clipped as it is for the data in the figure. One reason for the different power levels between the AGC-reference channel and other RX channels is that in the AGC reference channel an omnidirectional discone antenna is used whereas the antenna elements of the antenna group used at the TKK RX are directive antennas. The gain of the elements used in the TKK RX antenna group is about 7 dB (see Table 3.2). The reference antenna is vertically polarized, and so there is difference in the polarizations between the reference antenna and horizontally polarized RX channels, although in general this is not a problem, because in the transmission 45° slanted polarizations are used. In addition, the reference antenna was mounted so that in some situations the antenna group may shadow the reference antenna so that the difference in received power level grows even larger. Also another reason to the clipping rises from the AGC sampling. In the AGC system of the TKK RX the samples for determining the appropriate amount of attenuation are taken from the first part of each snapshot from a signle TX-RX pair. This is not a problem when the transmitter and receiver are fully synchronized, because then the samples are taken from the first TX channel, which has the omnidirectional discone antenna, but because now the TX and TKK RX are not fully synchronized, the TX channel these samples are taken from can not be known beforehand and it can be any of the TX channels. Thus the the TX channel that is transmitting while the AGC value is determined, could be pointing away from the receiver and thus the AGC

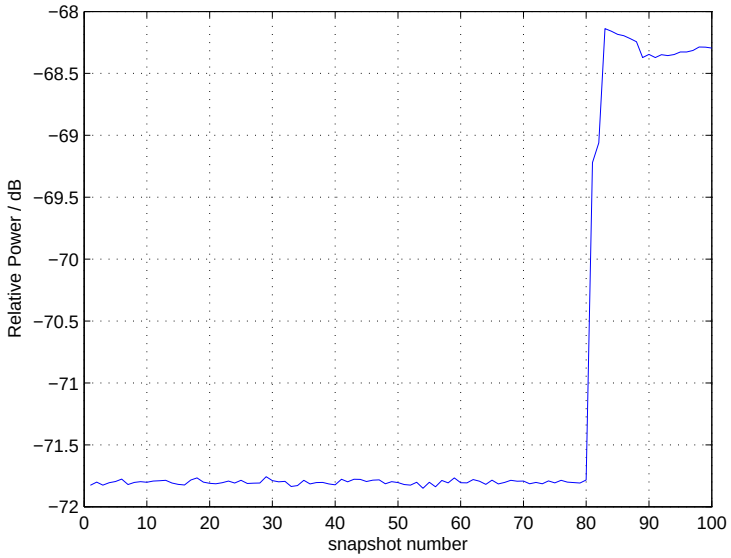

Figure 5.7: Average power of each snapshot from the beginning of a measurement, LU data

would be set to a too low value.

Fortunately there are some solutions for fixing the clipping issue. Using the new AGC system described in Section 3.1 would remove both of the two issues in the current AGC system, that cause the clipping. This is because in the new AGC system the signal level values for determining the correct attenuation value are taken randomly from all the RX channels and from a time period longer than a full MIMO snapshot, so that the AGC samples are taken from all the TX-RX pairs. Unfortunately the use of this newer system requires writing a new control program, and for time reasons, this has not been possible during this work. One possible solution would have been to modify the sampling of the current AGC-system by changing the program of the controlling computer, but also this would have been too time consuming.

One other solution would be to use a directive antenna at the reference channel of the TKK RX instead of an omnidirectional antenna. This would even out the difference in antenna gain between the reference antenna and the elements of the TKK RX antenna group. However when using a directive reference antenna, it's difficult to know how to direct the antenna, especially in NLOS measurements, and if the antenna does'not point to the direction of the strongest incoming signal, the use of directional reference antenna can make the clipping issue even worse.

Thus it was decided to reduce the clipping issue by reducing the difference of received power between the RX reference channel and other RX channels. This could have been done either by inserting an amplifier to the reference channel or attenuating the received signal before sampling, i.e. after the AGC chain. Because adding an amplifier would have also required adding additional RF filters, it was decided that it is easier to add the extra attenuators.

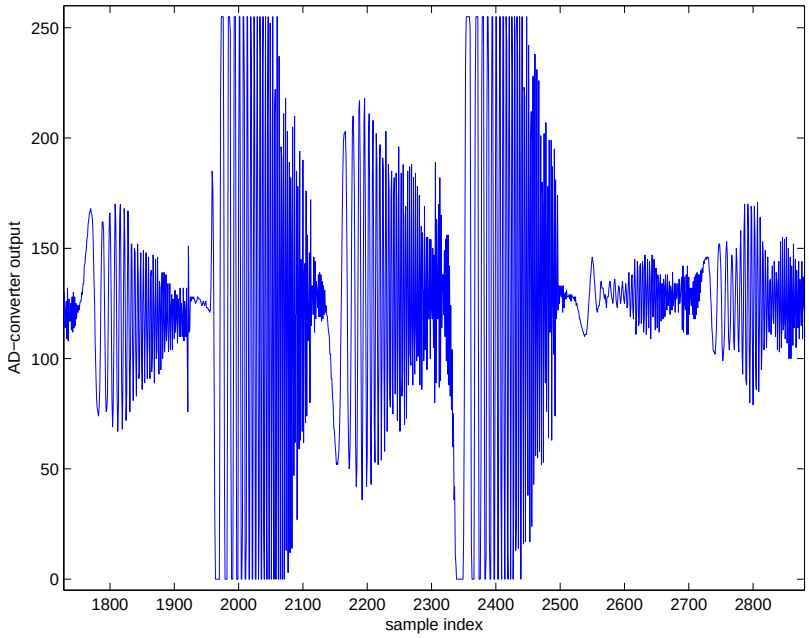

Figure 5.8: A section of I-channel raw data showing the effects of clipping

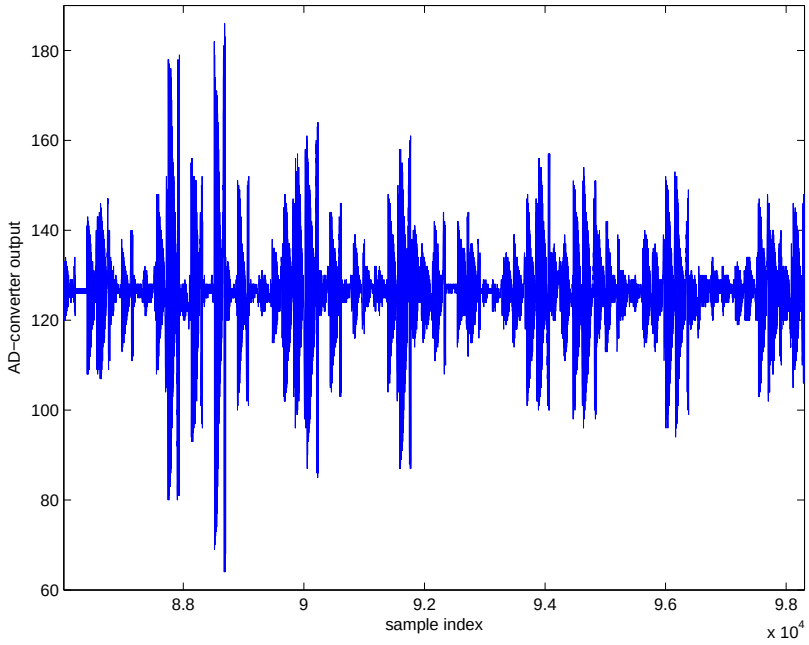

Figure 5.9: A section of I-channel raw data from the second measurement campaign

In a statistical analysis of the TKK data, it was noticed that in most of the measurements the clipping of the strongest channel, and so the maximum amount of clipping, was 10 dB on average. Thus 10 dB attenuators were added to both I and Q channels, in front of the sampling boards. This of course means that the dynamic range of the TKK RX is shifted by 10 dB. However because the attenuation is added after the AGC chain the sensitivity of the receiver is not affected.

These attenuators were used in the second measurement campaign, and in the results of that

campaign the described clipping issue was not detected. Figure 5.9 shows data containing one TX channel from the second measurement campaign and from a similar measurement than the data of Figures 5.4, 5.5 and 5.8. I't can bee seen that signal strength is good and well below the clipping limits, even though the data shown in the figure is from the strongest TX channel and from the strongest section of the scenario. Thus the clipping issue was succesfully solved.

5.6 Measurement Results

After the TKK data has been reordered (see Section5.3) and snapshot synchronization between the TKK and LU sounder data (see Section 5.4) has been done, the data is ready to be analyzed. Figure 5.10 shows PDPs of both the TKK and LU data from a corner-measurement scenario similar to the scenario represented in Figure 4.10. It can be noted that the two PDPs are very similiar although the behavior of the power is nearly reversed as a function of measurement time in the TKK receiver, because the TX was moved from LU RX to TKK RX. Thus the figure verifies that with the measurement setup presented in this thesis, impulse response of the dual-link channel can be measured. In Figure 5.11 some pathloss and delay spread results [109] are presented. Also some additional capacity results are presented in [109]. The data is from the same scenario as used to produce the PDPs in Figure 5.10, and as with the PDPs, we can see similiar behavior also in pathloss and delay spread between the two links, although in the LU RX, there are large values of delay spread in the transition area, in distance around 18 m, in which the TX goes from LOS to NLOS. This is due to the multiple reflections at the large hall, which are not present at the TKK RX because it was situated in the narrow corridor. So already from these first results we can see that using the data of the multi-link measurements done as a part of this thesis we can analyze the behavior of multi-link MIMO channels.

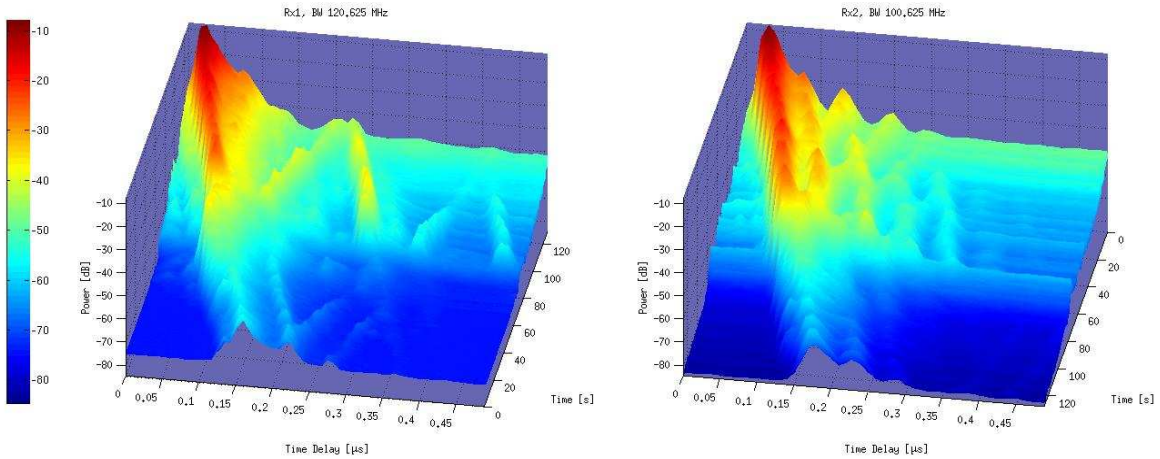

Figure 5.10: Power delay profiles measured with LU (on the left) and TKK (on the right) receivers

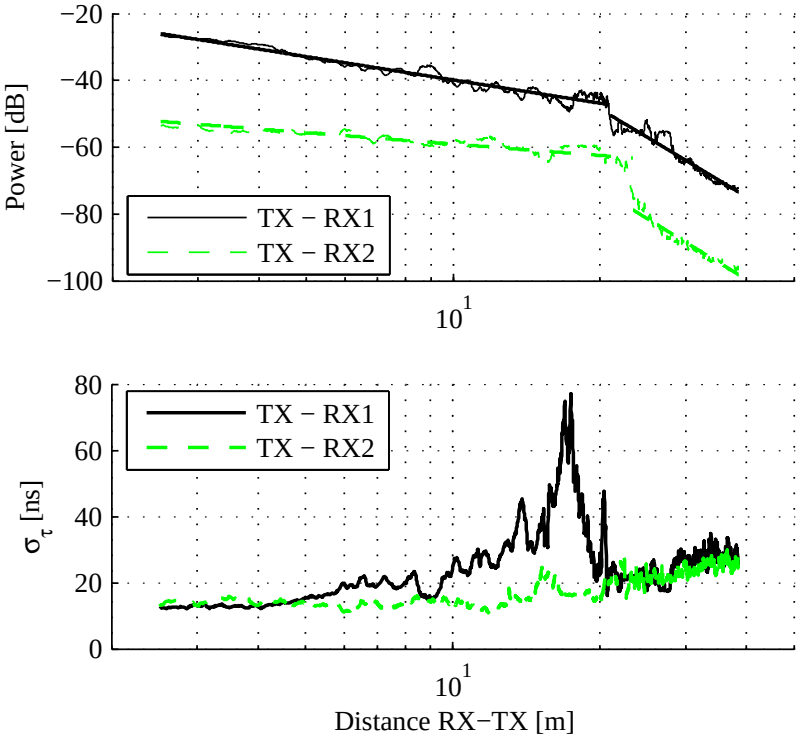

Figure 5.11: Pathloss and delay spread as functions of moving distance for the two links (RX1 is the LU RX and RX2 the TKK RX)

CHAPTER 6

Conclusions

In this thesis a measurement system for measuring simultaneously the dynamic wide-band multi-link MIMO channel at 5.3 GHz was developed. The measurement system consists of two separate channel sounders, and is able to measure 2x32x32 multi-link MIMO channels with maximum doppler frequency of 11,73 Hz. Large part of this thesis was to ensure the interoperability between these two sounders. Some modifications to the TKK sounder were made as a part of this thesis for achieving this interoperability. Even when full synchronization between the two sounders could not be achieved, the data sets of the two sounders can be combined for the analysis of multi-link MIMO channels with some post-processing.

A measurement campaign was conducted for testing the developed measurement system. After this measurement campaign, a clipping issue caused by the measurement system were found from the TKK measurement data. Although the issue hinders the utilization of the data, there are some sections of measurements that can be used. Modifications to the system were made and a second measurement campaign was conducted. It was found that the AGC issue that were noticed after the first measurement campaign was successfully fixed by the modifications, and so the second measurement campaign was successful.

In this thesis it was shown that the described measurement setup is able to record the impulse responses of dynamic multi-link MIMO channels, and so the data of the measurement campaigns can be used in analyzing this kind of channels. In addition to these PDP results, a delay spread and path loss charactheristics of a particular scenario were presented as an example.

The measurement setup described in this thesis, will be used in several measurement campaigns also in the future. Measurements in different kind of measurement environments and scenarios, including outdoor, indoor-to-outdoor and outdoor-to-indoor are planned. In addition to future measurements, a natural continuation for this work will be the analysis of the previous measurement data and developement of the stochastic multi-link model based on the measurement data.

Bibliography

[1] Y. Xiao, "IEEE 802.11n: Enhancements for higher throughput in wireless lans," *IEEE Magazine on Wireless Communications*, vol. 12, no. 6, pp. 82–91, December 2005.

[2] G. J. Foschini, "Layered space-time architecture for wireless communication in a fading enviroment when using multi-element antennas," *Bell Labs Technical Journal*, pp. 41–59, 1996.

[3] L. M. Correia, Ed., *Mobile Broadband Multimedia Networks Technigues, Models and Tools for 4G*. Academic Press, 2006.

[4] A. Paulraj, R. Nabar, and D. Gore, *Introduction to Space-Time Wireless Communications*. Cambridge University Press, 2003.

[5] R. Vaughan and J. Andersen, *Channels, Propagation and Antennas for Mobile Communications*. The Institution of Electrical Engineers, 2003.

[6] R. Thoma, M. Landmann, G. Sommerkorn, and A. Richter, "Multidimensional high-resolution channel sounding in mobile radio," in *Proceedings of the 21st IEEE Instrumentation and Measurement Technology Conference, IMTC 04.*, 2004.

[7] A. Richter, "Estimation of radio channel parameters: Models and algorithms," Ph.D. dissertation, Ilmenau University of Technology, Ilmenau, Germany, 2005.

[8] V. Degli-Esposti, "A diffuse scattering model for urban propagation prediction," *IEEE Transactions on Antennas and Propagation*, vol. 49, no. 7, pp. 1111–1113, July 2001.

[9] V. Degli-Esposti, D. Guiducci, A. de'Marsi, P. Azzi, and F. Fuschini, "An advanced field prediction model including diffuse scattering," *IEEE Transactions on Antennas and Propagation*, vol. 52, no. 7, pp. 1717–1728, July 2004.

[10] V. Erceg, "TGn channel models," IEEE 802.11-03/940r4, Tech. Rep., 2004.

[11] G. T. 25.996, "3rd Generation Partnership Project; technical specification group radio access network; spatial channel model for mimo simulations (release 6)," IEEE 802.11-03/940r4, Tech. Rep.

[12] D. Baum, J. Hansen, and J. Salo, "An interim channel model for beyond-3G systems: extending the 3GPP spatial channel model (SCM)," in *IEEE 61st Vehicular Technology Conference, 2005. VTC 2005-Spring. 2005*, vol. 5, 30 May-1 June 2005, pp. 3132–3136.

[13] H. El-Sallabi, D. Baum, P. Zetterberg, P. Kyosti, T. Rautiainen, and C. Schneider, "Wideband spatial channel model for MIMO systems at 5 GHz in indoor and outdoor environments," in *IEEE 63rd Vehicular Technology Conference, 2006. VTC 2006-Spring.*, vol. 6, 2006, pp. 2916 – 2921.

[14] M. Narandzic, C. Schneider, R. Thoma, T. Jamsa, P. Kyosti, and X. Zhao, "Comparison of SCM, SCME, and WINNER channel models," in *IEEE 65th Vehicular Technology Conference, 2007. VTC2007-Spring.*, 22-25 April 2007, pp. 413–417.

[15] J. Kermoal, L. Schumacher, K. Pedersen, P. Mogensen, and F. Frederiksen, "A stochastic MIMO radio channel model with experimental validation," *IEEE Journal on Selected Areas in Communications*, vol. 20, no. 6, pp. 1211–1226, Aug. 2002.

[16] V.-M. Kolmonen, J.-P. Kermoal, and P. Vainikainen, "Comparison of correlation-based and ray-based radio MIMO channel models," in *IEEE 17th International Symposium on Personal, Indoor and Mobile Radio Communications, 2006*, Sept. 2006, pp. 1–5.

[17] J. Kermoal, P. Mogensen, S. Jensen, J. Andersen, F. Frederiksen, T. Sorensen, and K. Pedersen, "Experimental investigation of multipath richness for multi-element transmit and receive antenna arrays," in *IEEE 51st Vehicular Technology Conference Proceedings, 2000. VTC 2000-Spring Tokyo. 2000*, vol. 3, 15-18 May 2000, pp. 2004–2008.

[18] C. Martin, J. Winters, and N. Sollenberger, "Multiple-input multiple-output (MIMO) radio channel measurements," in *52nd Vehicular Technology Conference, 2000. IEEE VTS-Fall VTC 2000.*, 2000.

[19] C. Martin, J. Winters, H. Zeng, N. Sollenberger, and A. Dixit, "Multiple-input multiple-output (MIMO) radio channel measurements and experimental implementation for EDGE," in *Conference Record of the Thirty-Fourth Asilomar Conference on Signals, Systems and Computers, 2000.*, vol. 1, 29 Oct.-1 Nov. 2000, pp. 738–742.

[20] S. Howard, H. Inanoglu, J. Ketchum, M. Wallace, and R. Walton, "Results from MIMO channel measurements," in *The 13th IEEE International Symposium on Personal, Indoor and Mobile Radio Communications, 2002.*, vol. 4, 15-18 Sept. 2002, pp. 1932–1936.

[21] M. Hunukumbure and M. Beach, "Outdoor MIMO measurements for UTRA applications," in *COST 273 TD(02)*, 2002. [Online]. Available: citeseer.ist.psu.edu/555311.html

[22] P. Kyritsi, D. Cox, R. Valenzuela, and P. Wolniansky, "Correlation analysis based on MIMO channel measurements in an indoor environment," *IEEE Journal on Selected Areas in Communications*, vol. 21, no. 5, pp. 713–720, June 2003.

[23] ——, "Effect of antenna polarization on the capacity of a multiple element system in an indoor environment," *IEEE Journal on Selected Areas in Communications*, vol. 20, no. 6, pp. 1227–1239, Aug. 2002.

[24] S. Salous, P. Filippidis, R. Lewenz, I. Hawkins, N. Razavi-Ghods, and M. Abdallah, "Parallel receiver channel sounder for spatial and MIMO characterisation of the mobile radio channel," in *IEE Proceedings-, Communications*, vol. 152, no. 6, 9 Dec. 2005, pp. 912–918.

[25] M. Hunukumbure and M. Beach, "MIMO channel measurements and analysis with prototype user devices in a 2GHz urban cell," in *The 17th Annual IEEE International Symposium on Personal, Indoor and Mobile Communications (PIMRC06)*, 2006.

[26] D. Shutin and G. Kubin, "Tracking direction-of-arrival for wireless communication with multiple antennas," in *4th IEEE Workshop on Signal Processing Advances in Wireless Communications, 2003. SPAWC 2003.*, 15-18 June 2003, pp. 422–426.

[27] J. Kermoal, L. Schumacher, P. Mogensen, and K. Pedersen, "Experimental investigation of correlation properties of MIMO radio channels for indoor picocell scenarios," in *52nd Vehicular Technology Conference, 2000. IEEE VTS-Fall VTC 2000.*, vol. 1, 24-28 Sept. 2000, pp. 14–21.

[28] J. Kermoal, L. Schumacher, F. Frederiksen, and P. Mogensen, "Polarization diversity in MIMO radio channels: experimental validation of a stochastic model and performance assessment," in *IEEE VTS 54th Vehicular Technology Conference, 2001. VTC 2001 Fall.*, vol. 1, 2001, pp. 22 – 26.

[29] D. Chizhik, J. Ling, P. Wolniansky, R. Valenzuela, N. Costa, and K. Huber, "Multiple-input-multiple-output measurements and modeling in manhattan," *IEEE Journal on Selected Areas in Communications*, vol. 21, no. 3, pp. 321–331, April 2003.

[30] H. Xu, M. Gans, D. Chizhik, J. Ling, P. Wolniansky, and R. Valenzuela, "Spatial and temporal variations of MIMO channels and impacts on capacity," in *IEEE International Conference on Communications, 2002. ICC 2002.*, vol. 1, 28 April-2 May 2002, pp. 262–266.

[31] J. Ling, D. Chizhik, P. Wolinansky, R. Valenzuela, N. Costa, and K. Huber, "MIMO measurement in manhattan," in *The 13th IEEE International Symposium on Personal, Indoor and Mobile Radio Communications, 2002.*, vol. 4, 15-18 Sept. 2002, pp. 1631–1635.

[32] J. Ling, D. Chizhik, P. Wolniansky, R. Valenzuela, N. Costa, and K. Huber, "Multiple transmit multiple receive (MTMR) capacity survey in manhattan," in *Electronics Letters*, vol. 37, no. 16, 2 Aug. 2001, pp. 1041–1042. [Online]. Available: http://ieeexplore.ieee.org/xpls/abs_all.jsp?isnumber=20388\&arnumber=941820\&type=ref

[33] J. Kivinen, P. Suvikunnas, L. Vuokko, and P. Vainikainen, "Experimental investigations of MIMO propagation channels," in *IEEE Antennas and Propagation Society International Symposium, 2002.*, vol. 3, 16-21 June 2002, p. 206.

[34] K. Sulonen, P. Suvikunnas, L. Vuokko, J. Kivinen, and P. Vainikainen, "Comparison of MIMO antenna configurations in picocell and microcell environments," *IEEE Journal on Selected Areas in Communications*, vol. 21, no. 5, pp. 703–712, June 2003.

[35] E. Jaramillo, O. Fernadez, and R. Torres, "Empirical analysis of 2& outdoor-indoor MIMO channels for FBWA applications," in *IEEE Mediterranean Electrotechnical Conference, 2006. MELECON 2006.*, 16-19 May 2006, pp. 617–621.

[36] V. Anreddy and M. Ingram, "Capacity of measured ricean and rayleigh indoor MIMO channels at 2.4 GHz with polarization and spatial diversity," in *IEEE Wireless Communications and Networking Conference, 2006. WCNC 2006.*, vol. 2, 3-6 April 2006, pp. 946–951.

[37] B. Maharaj, J. Wallace, L. Linde, and M. Jensen, "Linear dependence of double-directional spatial power spectra at 2.4 and 5.2 GHz from indoor MIMO channel measurements," in *Electronics Letters*, vol. 41, no. 24, 24 Nov. 2005, pp. 1338–1340.

[38] ——, "Frequency scaling of spatial correlation from co-located 2.4 and 5.2 GHz wideband indoor MIMO channel measurements," in *Electronics Letters*, vol. 41, no. 6, 17 March 2005, pp. 336–337.

[39] J. Wallace and M. Jensen, "Measurement and characterization of the time variation of indoor and outdoor MIMO channels at 2.4 and 5.2 GHz," in *IEEE 62nd Vehicular Technology Conference, 2005. VTC-2005-Fall. 2005*, vol. 2, 25-28 Sept., 2005, pp. 1289–1293.

[40] T. Svantesson and J. Wallace, "Statistical characterization of the indoor MIMO channel based on LOS/NLOS measurements," in *Conference Record of the Thirty-Sixth Asilomar Conference on Signals, Systems and Computers, 2002.*, vol. 2, 3-6 Nov. 2002, pp. 1354–1358.

[41] H. Xu, M. Gans, N. Amitay, R. Valenzuela, T. Sizer, R. Storz, D. Taylor, M. McDonald, and C. Tran, "MIMO channel capacity for fixed wireless: measurements and models," in *IEEE VTS 54th Vehicular Technology Conference, 2001. VTC 2001 Fall.*, vol. 2, 7-11 Oct. 2001, pp. 1068–1072.

[42] J. Wallace and M. Jensen, "Spatial characteristics of the MIMO wireless channel: experimental data acquisition and analysis," in *IEEE International Conference on Acoustics, Speech, and Signal Processing, 2001. Proceedings. (ICASSP '01). 2001*, vol. 4, 7-11 May 2001, pp. 2497–2500.

[43] ——, "Characteristics of measured 4& and 10&0 MIMO wireless channel data at 2.4-GHz," in *IEEE Antennas and Propagation Society International Symposium, 2001.*, vol. 3, 8-13 July 2001, pp. 96–99.

[44] J. Wallace, M. Jensen, A. Swindlehurst, and B. Jeffs, "Experimental characterization of the MIMO wireless channel: data acquisition and analysis," *IEEE Transactions on Wireless Communications*, vol. 2, no. 2, pp. 335–343, March 2003.

[45] J. W. Wallace, "Modeling electromagnetic wave propagation in electrically large structures," Ph.D. dissertation, Department of Electrical and Computer Engineering, Birgham Young University, April 2002.

[46] J. Wallace and M. Jensen, "Modeling the indoor MIMO wireless channel," *IEEE Transactions on Antennas and Propagation*, vol. 50, no. 5, pp. 591–599, May 2002.

[47] A. Knopp, M. Chouayakh, and B. Lankl, "MIMO-capacities for broadband in-room quasi-deterministic line-of-sight radio channels derived from measurements," in *The 17th Annual IEEE International Symposium on Personal, Indoor and Mobile Communications (PIMRC06)*, 2006.

[48] Z. Tang and A. S. Mohan, "Experimental investigation of indoor MIMO ricean channel capacity," *IEEE Antennas and Wireless Propagation Letters*, vol. Vol. 4, pp. 55–58, 2005.

[49] J. Kolu, T. Jamsa, and A. Hulkkonen, "Real time simulation of measured radio channels," in *IEEE 58th Vehicular Technology Conference, 2003. VTC 2003-Fall. 2003*, vol. 1, 6-9 Oct. 2003, pp. 183–187.

[50] M. Stoytchev and H. Safar, "Statistics of the MIMO radio channel in indoor environments," in *IEEE VTS 54th Vehicular Technology Conference, 2001. VTC 2001 Fall.*, vol. 3, 7-11 Oct. 2001, pp. 1804–1808.

[51] D. Laselva, X. Zhao, J. Meinila, T. Jamsa, J. Nuutinen, P. Kyosti, and L. Hentila, "Empirical models and parameters for rural and indoor wideband radio channels at 2.45 and 5.25 ghz," in *IEEE 16th International Symposium on Personal, Indoor and Mobile Radio Communications, 2005. PIMRC 2005.*, vol. 1, 11-14 Sept. 2005, pp. 654–658.

[52] V. Erceg, P. Soma, D. Baum, and A. Paulraj, "Capacity obtained from multiple-input multiple-output channel measurements in fixed wireless environments at 2.5 GHz," in *IEEE International Conference on Communications, 2002. ICC 2002.*, vol. 1, 28 April-2 May 2002, pp. 396–400.

[53] V. Erceg, P. Soma, D. Baum, and S. Catreux, "Multiple-input multiple-output fixed wireless radio channel measurements and modeling using dual-polarized antennas at 2.5 GHz," *IEEE Transactions on Wireless Communications*, vol. 3, no. 6, pp. 2288–2298, Nov. 2004.

[54] P. Soma, D. Baum, V. Erceg, R. Krishnamoorthy, and A. Paulraj, "Analysis and modeling of multiple-input multiple-output (MIMO) radio channel based on outdoor

measurements conducted at 2.5 GHz for fixed BWA applications," in *IEEE International Conference on Communications, 2002. ICC 2002.*, vol. 1, 28 April-2 May 2002, pp. 272–276.

[55] M. Batariere, T. Blankenship, J. Kepler, T. Krauss, I. Lisica, S. Mukthavaram, J. Porter, T. Thomas, and F. Vook, "Wideband MIMO mobile impulse response measurements at 3.7 GHz," in *IEEE 55th Vehicular Technology Conference, 2002. VTC Spring 2002.*, vol. 1, 6-9 May 2002, pp. 26–30.

[56] T. Mitsui, M. Otani, C. Eugene, and K. Sakaguchi, "Indoor MIMO channel measurements for evaluation of effectiveness of array antenna configurations," in *IEEE 58th Vehicular Technology Conference, 2003. VTC 2003-Fall. 2003*, vol. 1, 6-9 Oct. 2003, pp. 84–88.

[57] T. Rautiainen, K. Kalliola, and J. Juntunen, "Wideband radio propagation characteristics at 5.3 GHz in suburban environments," in *IEEE 16th International Symposium on Personal, Indoor and Mobile Radio Communications, 2005. PIMRC 2005.*, vol. 2, 11-14 Sept. 2005, pp. 868–872.

[58] T. Fugen, G. Sommerkorn, J. Maurer, D. Hampicke, W. Wiesbeck, and R. Thoma, "MIMO capacities for different antenna arrangements based on double directional wide-band channel measurements," in *The 13th IEEE International Symposium on Personal, Indoor and Mobile Radio Communications, 2002.*, vol. 4, 15-18 Sept. 2002, pp. 1777–1781.

[59] D. Hampicke, C. Schneider, M. Landmann, A. Richter, G. Sommerkorn, and R. Thoma, "Measurement-based simulation of mobile radio channels with multiple antennas using a directional parametric data model," in *IEEE VTS 54th Vehicular Technology Conference, 2001. VTC 2001 Fall.*, vol. 2, 7-11 Oct. 2001, pp. 1073–1077.

[60] D. Hampicke, M. Landmann, C. Schneider, G. Sommerkorn, T. Thoma, T. Fugen, J. Maurer, and W. Wiesbeck, "MIMO capacities for different antenna array structures based on double directional wide-band channel measurements," in *IEEE 56th Vehicular Technology Conference, 2002. Proceedings. VTC 2002-Fall. 2002*, vol. 1, 24-28 Sept. 2002, pp. 180–184.

[61] C. Tan, C. Chin, M. Sim, and M. Beach, "Modelling the general dependency between directions of arrival and departure for an indoor MIMO channel," in *IEEE 63rd Vehicular Technology Conference, 2006. VTC 2006-Spring.*, vol. Volume 6, 2006, pp. 2878 – 2882.

[62] L. Thiele, M. Peter, and V. Jungnickel, "Statistics of the ricean k-factor at 5.2 GHz in an urban macro-cell scenario," in *The 17th Annual IEEE International Symposium on Personal, Indoor and Mobile Communications (PIMRC06)*, 2006.

[63] R. Thoma, D. Hampicke, M. Landmann, G. Sommerkorn, and A. Richter, "MIMO measurement for double-directional channel modelling," in *IEE Seminar on MIMO:*

Communications Systems from Concept to Implementations (Ref. No. 2001/175), 12 Dec. 2001, pp. 1/1–1/7.

[64] K. Yu, M. Bengtsson, B. Ottersten, D. McNamara, P. Karlsson, and M. Beach, "Second order statistics of NLOS indoor MIMO channels based on 5.2 GHz measurements," in *IEEE Global Telecommunications Conference, 2001. GLOBECOM '01.*, vol. 1, 25-29 Nov. 2001, pp. 156–160.

[65] N. Czink, E. Bonek, X. Yin, and B. Fleury, "Cluster angular spreads in a MIMO indoor propagation environment," in *IEEE 16th International Symposium on Personal, Indoor and Mobile Radio Communications, 2005. PIMRC 2005.*, vol. 1, 11-14 Sept. 2005, pp. 664–668. [Online]. Available: http://ieeexplore.ieee.org/iel5/10989/34626/01651519.pdf?tp=\&arnumber=1651519\&isnumber=34626

[66] N. Czink, M. Herdin, H. Ozcelik, and E. Bonek, "Number of multipath clusters in indoor MIMO propagation environments," in *Electronics Letters*, vol. 40, no. 23, 11 Nov. 2004, pp. 1498–1499.

[67] M. Herdin, H. Ozcelik, H. Hofstetter, and E. Bonek, "Linking reduction in measured MIMO capacity with dominant-wave propagation," in *10th International Conference on Telecommunications, 2003. ICT 2003.*, vol. 2, 23 Feb.-1 March 2003, pp. 1526–1530.

[68] ——, "Variation of measured indoor MIMO capacity with receive direction and position at 5.2 GHz," in *Electronics Letters*, vol. 38, no. 21, 10 Oct. 2002, pp. 1283–1285.

[69] D. McNamara, M. Beach, and P. Fletcher, "Experimental investigation of the temporal variation of MIMO channels," in *Vehicular Technology Conference, 2001. VTC 2001 Fall. IEEE VTS 54th*, vol. 2, 7-11 Oct. 2001, pp. 1063–1067.

[70] D. McNamara, M. Beach, P. Fletcher, and P. Karlsson, "Temporal variation of multiple-input multiple-output (MIMO) channels in indoor environments," in *Eleventh International Conference on Antennas and Propagation, 2001. (IEE Conf. Publ. No. 480)*, vol. 2, 17-20 April 2001, pp. 578–582.

[71] ——, "Capacity variation of indoor multiple-input multiple-output channels," in *Electronics Letters*, vol. 36, no. 24, 23 Nov 2000, pp. 2037–2038.

[72] ——, "Initial investigation of multiple-input multiple-output (MIMO) channels in indoor environments," in *Symposium on Communications and Vehicular Technology, 2000. SCVT-200.*, 19 Oct. 2000, pp. 139–143.

[73] D. McNamara, M. Beach, P. Karlsson, and P. Fletcher, "Initial characterisation or multiple-input multiple-output (MIMO) channels for space-time communication," in *52nd Vehicular Technology Conference, 2000. IEEE VTS-Fall VTC 2000.*, vol. 3, 24-28 Sept. 2000, pp. 1193–1197.

[74] A. Molisch, M. Steinbauer, M. Toeltsch, E. Bonek, and R. Thoma, "Capacity of MIMO systems based on measured wireless channels," *IEEE Journal on Selected Areas in Communications*, vol. 20, no. 3, pp. 561–569, April 2002.

[75] M. Steinbauer, D. Hampicke, G. Sommerkorn, A. Schneider, A. Molisch, R. Thoma, and E. Bonek, "Array measurement of the double-directional mobile radio channel," in *IEEE 51st Vehicular Technology Conference Proceedings, 2000. VTC 2000-Spring Tokyo. 2000*, vol. 3, 15-18 May 2000, pp. 1656–1662.

[76] M. Steinbauer, A. Molisch, and E. Bonek, "The double-directional radio channel," *IEEE Antennas and Propagation Magazine*, vol. 43, no. 4, pp. 51–63, Aug. 2001.

[77] H. Ozcelik, M. Herdin, H. Hofstetter, and E. Bonek, "A comparison of measured 8 /spl times/ 8 MIMO systems with a popular stochastic channel model at 5.2 GHz," in *10th International Conference on Telecommunications, 2003. ICT 2003.*, vol. 2, 23 Feb.-1 March 2003, pp. 1542–1546.

[78] N. Skentos, A. Kanatas, G. Pantos, and P. Constantinou, "Capacity results from short range fixed MIMO measurements at 5.2 GHz in urban propagation environment," in *IEEE International Conference on Communications, 2004*, vol. 5, 20-24 June 2004, pp. 3020–3024.

[79] N. Skentos, A. Kanatas, and P. Constantinou, "MIMO channel characterization results from short range rooftop to rooftop wideband measurements," in *IEEE International Conference on Wireless And Mobile Computing, Networking And Communications, 2005. (WiMob'2005)*, vol. 1, 22-24 Aug. 2005, pp. 137–144.

[80] J. Wallace, H. Ozcelik, M. Herdin, E. Bonek, and M. Jensen, "Power and complex envelope correlation for modeling measured indoor MIMO channels: a beamforming evaluation," in *IEEE 58th Vehicular Technology Conference, 2003. VTC 2003-Fall. 2003*, vol. 1, 6-9 Oct. 2003, pp. 363–367.

[81] H. Özcelik, "Indoor MIMO channel models," Ph.D. dissertation, Institut für Nachrichtentechnik und Hochfrequenztechnik, Technische Universität Wien, Vienna, Austria, December 2004. [Online]. Available: http://www.nt.tuwien.ac.at/mobile/theses_finished/

[82] H. Özcelik, M. Herdin, R. Prestros, and E. Bonek, "How MIMO capacity is linked with single element fading statistics," in *International Conference on Elegtromagnetics in Advanced Applications, Torino, Italy*, September 2003, pp. 775–778. [Online]. Available: http://publik.tuwien.ac.at/files/pub-et_7145.pdf

[83] S. Wyne, P. Almers, G. Eriksson, J. Karedal, F. Tufvesson, and A. Molisch, "Outdoor to indoor office MIMO measurements at 5.2 GHz," in *IEEE 60th Vehicular Technology Conference, 2004. VTC2004-Fall. 2004*, vol. 1, 26-29 Sept. 2004, pp. 101–105.

[84] S. Wyne, A. Molisch, P. Almers, G. Eriksson, J. Karedal, and F. Tufvesson, "Statistical evaluation of outdoor-to-indoor office MIMO measurements at 5.2 GHz," in *IEEE 61st Vehicular Technology Conference, 2005. VTC 2005-Spring. 2005*, vol. 1, 30 May-1 June 2005, pp. 146–150.

[85] K. Yu, M. Bengtsson, B. Ottersten, D. McNamara, P. Karlsson, and M. Beach, "A wideband statistical model for NLOS indoor MIMO channels," in *IEEE 55th Vehicular Technology Conference, 2002. VTC Spring 2002.*, vol. 1, 6-9 May 2002, pp. 370–374.

[86] ——, "Modeling of wide-band MIMO radio channels based on NLoS indoor measurements," *IEEE Transactions on Vehicular Technology*, vol. 53, no. 3, pp. 655–665, May 2004.

[87] T. Zwick, D. Hampicke, J. Maurer, A. Richter, G. Sommerkorn, R. Thoma, and W. Wiesbeck, "Results of double-directional channel sounding measurements," in *IEEE 51st Vehicular Technology Conference Proceedings, 2000. VTC 2000-Spring Tokyo. 2000*, vol. 3, 15-18 May 2000, pp. 2497–2501.

[88] D. McNamara, M. Beach, and P. Fletcher, "Spatial correlation in indoor MIMO channels," in *The 13th IEEE International Symposium on Personal, Indoor and Mobile Radio Communications, 2002.*, vol. 1, 15-18 Sept. 2002, pp. 290–294.

[89] A. Richter, D. Hampicke, G. Sommerkorn, and R. Thoma, "MIMO measurement and joint M-D parameter estimation of mobile radio channels," in *IEEE VTS 53rd Vehicular Technology Conference, 2001. VTC 2001 Spring.*, vol. 1, 6-9 May 2001, pp. 214–218.

[90] C. Eugene, K. Sakaguchi, and K. Araki, "Experimental and analytical investigation of MIMO channel capacity in an indoor line-of-sight (LOS) environment," in *15th IEEE International Symposium on Personal, Indoor and Mobile Radio Communications, 2004. PIMRC 2004.*, vol. 1, 5-8 Sept. 2004, pp. 295–300.

[91] J. Ling, D. Chizhik, D. Samardzija, and R. Valenzuela, "Wideband and MIMO measurements in wooded and open areas," in *IEEE Antennas and Propagation Society International Symposium, 2005*, vol. 3B, 3-8 July 2005, pp. 422–425.

[92] A. Intarapanich, P. Kafle, R. Davies, A. Sesay, and J. McRory, "Spatial correlation measurements for broadband MIMO wireless channels," in *IEEE 60th Vehicular Technology Conference, 2004. VTC2004-Fall. 2004*, vol. 1, 26-29 Sept. 2004, pp. 52–56.

[93] R. Stridh, K. Yu, B. Ottersten, and P. Karlsson, "MIMO channel capacity and modeling issues on a measured indoor radio channel at 5.8 GHz," *IEEE Transactions on Wireless Communications*, vol. 4, no. 3, pp. 895–903, May 2005.

[94] J. B. Andersen, J. Ø. Nielsen, G. Bauch, and M. Herdin, "The large office environment-measurement and modeling of the wideband radio channel," in *The 17th Annual*

IEEE International Symposium on Personal, Indoor and Mobile Communications (PIMRC06), 2006.

[95] J. Nielsen, J. Andersen, P. Eggers, G. Pedersen, K. Olesen, and H. Suda, "Measurements of indoor 16/spl times/32 wideband MIMO channels at 5.8 GHz," in *IEEE Eighth International Symposium on Spread Spectrum Techniques and Applications, 2004*, 30 Aug.-2 Sept. 2004, pp. 864–868.

[96] R. Stridh and B. Ottersten, "Spatial characterization of indoor radio channel measurements at 5 GHz," in *Proceedings of the 2000 IEEE Sensor Array and Multichannel Signal Processing Workshop. 2000.*, 16-17 March 2000, pp. 58–62.

[97] J.-S. Jiang and M. Ingram, "Comparison of beam selection and antenna selection techniques in indoor MIMO systems at 5.8 GHz," in *Radio and Wireless Conference, 2003. RAWCON '03. Proceedings*, 10-13 Aug. 2003, pp. 179–182.

[98] K. Haneda and J. Takada, "High-resolution estimation of NLOS indoor MIMO channel with network analyzer based system," in *14th IEEE Proceedings on Personal, Indoor and Mobile Radio Communications, 2003. PIMRC 2003.*, vol. 1, 7-10 Sept. 2003, pp. 675–679.

[99] G. Janssen and J. Vriens, "High resolution coherent radio channel measurements using direct sequence spread spectrum modulation," in *6th Mediterranean Electrotechnical Conference, 1991. Proceedings., May 1991*, vol. 1, 1991, pp. 720 – 727.

[100] R. Thoma, D. Hampicke, A. Richter, G. Sommerkorn, A. Schneider, U. Trautwein, and W. Wirnitzer, "Identification of time-variant directional mobile radio channels," *IEEE Transactions on, Instrumentation and Measurement*, vol. 49, no. 2, pp. 357–364, April 2000.

[101] J. Kivinen, T. Korhonen, P. Aikio, R. Gruber, P. Vainikainen, and S.-G. Haggman, "Wideband radio channel measurement system at 2 ghz," *IEEE Transactions on Instrumentation and Measurement*, vol. 48, no. 1, pp. 39–44, Feb. 1999.

[102] J. Kivinen, P. Suvikunnas, D. Perez, C. Herrero, K. Kalliola, and P. Vainikainen, "Characterization system for mimo channels," in *Proceedings of 4th International Symposium on Wideband Personal Multimedia Communications conference, WPMC'01*, 9-12 September 2001, pp. 159–162.

[103] V.-M. Kolmonen, "Kolmiulotteinen 5 GHz:n MIMO-kanavaluotaimen antennijärjestelmä (Three-dimensional antenna system for 5 GHz MIMO channel sounder, in finnish)," Master's thesis, Teknillinen korkeakoulu, 2004.

[104] V.-M. Kolmonen, J. Kivinen, L. Vuokko, and P. Vainikainen, "5.3-GHz MIMO radio channel sounder," *IEEE Transactions on Instrumentation and Measurement*, vol. 55, no. 4, pp. 1263–1269, Aug. 2006.

[105] S. Ranvier, J. Kivinen, and P. Vainikainen, "Development of a 60 ghz mimo radio channel measurement system," in *Proceedings of the IEEE Instrumentation and Measurement Technology Conference, 2005*, vol. 3, 16-19 May 2005, pp. 1878–1882.

[106] C. Balanis, *Antenna Theory Analysis and Design.* John Wiley & Sons, 1997.

[107] N. Leo and M. Gunnarson, "Design och implementation av array-antenner för MIMO-mätningar (design and implementation of array antennas for mimo measurements, in swedish)," Master's thesis, Lunds Tekniska Högskola, 2005.

[108] P. Iversen, P. Garreau, and D. Burrell, "Real-time spherical near-field handset antenna measurements," *IEEE, Antennas and Propagation Magazine*, vol. 43, no. 3, pp. 90–94, June 2001.

[109] J. Koivunen, P. Almers, V.-M. Kolmonen, J. Salmi, A. Richter, F. Tufvesson, P. Suvikunnas, A. Molisch, and P. Vainikainen, "Dynamic multi-link indoor MIMO measurements at 5.3 GHz," in *Proceedings of the 2nd European Conference on Antennas and Propagation (EuCAP 2007)*, Edinburgh, 2007.

A MIMO Measurement Survey

Table 1: MIMO measurements
VA = Virtual Array, D = Dynamic, S = Static, DD = Double-Directional evaluation, PM = Parametrized model, y = yes, n = no, blank or na = not available

f (GHz)	BW (MHz)	D / S	Environment	LOS/NLOS	Cell size	MIMO setup	TX-geom	RX geom	TX-antenna	RX antenna	DD	PM	Reference
1,712	5	D	outdoor-indoor			4x4	UCA(VA)	ULA	V-dipole	dual-pol.	n	n	[17]
1,712 & 2,05	NB	D	outdoor-indoor & indoor	LOS & NLOS		4x4	UCA(VA) & interleaved array	ULA		v-pol. sleeve	y	y	[15]
1,9	0,03	D	indoor & outdoor			4x4			monopole	monopole	n	n	[18, 19]
1,9	3,5	D	urban & suburban			4x4	2x2	2x2	directive dual-pol.	directive dual-pol.	n	n	[20]
1,92	20		outdoor	LOS & NLOS	Micro	4x8					n	n	[21]
1,95	0,03	S	indoor		pico	12x15	4x4	4x4	directive	directive	n	n	[22, 23]
1,95	60	S	indoor & outdoor	NLOS		2x8 & 4x8	various	various	various	various	n	n	[24]
2	20	D	outdoor			4x4	various	various	various	various	n	n	[25]
2	120	D	outdoor	LOS		15x8	UCA	ULA			y	n	[26]
2,05	NB	D	indoor		pico	4x4	ULA	ULA	v-pol sleeve-dipole	v-pol sleeve-dipole	y	y	[27]
2,05	NB	D	indoor	LOS & NLOS	pico	2x4		ULA	dual-pol.		n	y	[28]
2,11	0,003		urban			16x16	8x2	8x2	8xV 8xP	8xV 8xP	y	y	[29, 30]
2,11	0,0032	D	urban	LOS & NLOS		16x16	2x8(dual-pol.)	2x8(dual-pol.)	directive	directive	n	n	[31, 32]
2,15	30	D	outdoor			16x64	ULA	spherical	directional, dual-pol.	directional, dual-pol.	n	n	[33]
2,15	30	D	indoor & outdoor		pico & micro	16x64	horizontal zigzag, LA	spherical	directive, dual-pol.	directive, dual-pol.	y	n	[34]
2,4	na (NB?)	S	outdoor-indoor	LOS & NLOS		2x2		VA	directive	omnidir.	n	n	[35]
2,4		S	Indoor		pico	4x4 and 2x2	5x5x2(VA)	5x5x2(VA)	dual-pol.	dual-pol.	n	n	[36]
2,4 & 5,2	80	S	indoor	NLOS	pico	8x8	UCA	UCA	monopole	monopole	y	n	[37]
2,4 & 5,2	80	S	indoor	NLOS	pico	8x8	ULA	ULA	V-pol monopole	V-pol monopole	y	n	[38]
2,4 & 5,2	100	D	indoor &outdoor			8x8	UCA	UCA	monopole	monopole	y	y	[39]
2,43		D	indoor	LOS & NLOS	pico	10x10	UCA	UCA	monopole	monopole	y	n	[40]
2,44	NB	S	outdoor-indoor			5x7	ULA	cross	directive	directive	n	n	[41]
2,45	0,025	S	indoor		pico	4x4 & 10x10	ULA	ULA	patch & monopole	patch & monopole	y	y	[42–45]
2,45	0,025	S	indoor	LOS & NLOS	pico	4x4 & 10x10	ULA	ULA	patch & monopole	patch & monopole	y	y	[46]
2,45	80	S	indoor	LOS & NLOS	Pico	5x5	ULA	ULA	dipole	dipole	y	n	[47]
2,45	120	S	indoor	LOS & OLOS	pico	4x4	UCA(VA)	URA(VA)	sleeve-dipole	sleeve-dipole	n	n	[48]
2,45		D	outdoor			28x16	Cylindrical	4x4	dual-pol. patch	dual-pol. patch	y	n	[49]
2,45		S	indoor	LOS & OLOS	pico	16x16	4x4	4x4	V-pol	V-pol	n	n	[50]

Table 1: MIMO measurements
VA = Virtual Array, D = Dynamic, S = Static, DD = Double-Directional evaluation, PM = Parametrized model, y = yes, n = no, blank or na = not available

f (GHz)	BW (MHz)	D / S	Environment	LOS/NLOS	Cell size	MIMO setup	TX-geom	RX geom	TX-antenna	RX antenna	DD	PM	Reference
2,45 & 5,25	100	D	rural & in-door	LOS & NLOS					dual-pol.	dual-pol.	n	y	[51]
2,48	4	S	suburban		Macro	2x2			directive	directive	n	n	[52]
2,48	4	S	suburban		Macro	2x2			directive	directive	n	y	[53]
2,5	4	S	suburban	LOS	macro	2x2			directive	slanted pol.	n	y	[54]
3,676	20	D	suburban			2x2			directive	omnidir.	n	n	[55]
5,2	16	S	indoor	NLOS	pico	4x4	ULA (VA)	ULA (VA)			n	n	[56]
5,2	100	D	suburban	LOS & NLOS	micro	4x4	4x4	2x2	dual-pol. patch		n	n	[57]
5,2	120	D	outdoor	LOS	micro	8beam x 8beam	CUBA	CUBA			y	n	[58]
5,2	120	D	outdoor		Micro	8beam x 8	CUBA	ULA			y	y	[59]
5,2	120	D	outdoor		Micro	8beam x 8beam	CUBA	CUBA			y	y	[60]
5,2	120	D	indoor	LOS & NLOS	pico	16x16	UCA	UCA	dual-pol. patch	dual-pol. patch	y	y	[61]
5,2	120	D	urban		macro	10x8	cube-antenna	UCA	dual-pol. patch	dual-pol. patch	n	y	[62]
5,2	120	D	outdoor			8x8	CUBA	CUBA	directive	directive	y	y	[63]
5,2	120	D	indoor	NLOS	pico	8x8	ULA	ULA	omnidir.	directive	n	y	[64]
5,2	120	S	indoor	LOS & NLOS	Pico	200x8	20x10 (VA)	ULA		directive	y	n	[65–68]
5,2	120	S		LOS & NLOS		8x8	ULA	ULA	monopole	V-pol. dipole-like	y	n	[69–73]
5,2	120	S	outdoor	LOS & NLOS	micro	16x8	2x8 (VA)	ULA	monopole		y	y	[74–76]
5,2	120	S	indoor	NLOS	pico	8x8	20x10 VA	ULA	monopole	patch	n	n	[77]
5,2	120	S	street-rooftop	LOS	micro	8x8	ULA	ULA	vert dipole	vert. dipole	n	n	[78]
5,2	120	S	rooftop-rooftop	LOS	micro	8x8	ULA	ULA	vert dipole	vert. dipole	y	n	[79]
5,2	120	S	indoor	LOS & NLOS	pico	200x8	20x10(VA)	ULA	monopole		y	y	[80–82]
5,2	120	S	outdoor-indoor	LOS & OLOS		8x16	ULA	UCA	dual-pol.	V-pol. monopole	y	n	[83, 84]
5,2	120	S	indoor	NLOS	pico	8x8	ULA	ULA	omnidir.	directive	n	y	[85]
5,2	120	S	indoor	NLOS	pico	8x8	ULA	ULA	omnidir.	omnidir.	n	y	[86]
5,2	120	S	outdoor	LOS		8beam x 8	multibeam	ULA	biconical multibeam	directive	y	n	[87]
5,2	120		indoor		pico	8x8	ULA	ULA	v-pol., monopole	v-pol.,dipole, directive	n	n	[88]
5,2	120		outdoor		micro	8x64	CUBA	8x8 URA			y	n	[89]
5,2			indoor	LOS	pico	4x4	ULA	ULA	Vertical sleeve dipole	Vertical sleeve dipole	n	y	[90]
5,5	6 & 0,003	D	rural	LOS		1x4 & 2x2			dual- & single-pol.	dual- & single-pol.	n	n	[91]
5,66	200		indoor	LOS & NLOS	Pico	4x4	ULA	ULA	monopole	monopole	y	y	[92]
5,8	60	S	indoor		pico	7x21	VA	VA	monopole	monopole	n	y	[93]
5,8	100	S	Indoor		Pico	16x32	4x4	4x8	monopole	monopole	y	y	[94]

Table 1: MIMO measurements
VA = Virtual Array, D = Dynamic, S = Static, DD = Double-Directional evaluation, PM = Parametrized model, y = yes, n = no, blank or na = not available

f (GHz)	BW (MHz)	D / S	Environment	LOS/NLOS	Cell size	MIMO setup	TX-geom	RX geom	TX-antenna	RX antenna	DD	PM	Reference
5,8	100	S & D	indoor	LOS & NLOS	pico	16x32	8x8 (4x4 active)	8x12 (4x8 active)	monopole	monopole	n	n	[95]
5,8	400	S	indoor		pico	7x21	VA	VA	monopole	monopole	n	n	[96]
5,8	500	S	indoor	LOS & NLOS	Pico	16x4	4x4 (VA)	ULA (VA)			n	n	[97]
5,85	100		indoor	NLOS	pico	10x49	UCA	7x7 URA (VA)			y	n	[98]